Journal of Medical Virology 79:811–819 (2007)

Prophylactic Effects of Chitin Microparticles on Highly Pathogenic H5N1 Influenza Virus

Takeshi Ichinohe,[1,2†] Noriyo Nagata,[1] Peter Strong,[3] Shin-ichi Tamura,[1] Hidehiro Takahashi,[1] Ai Ninomiya,[4] Masaki Imai,[4] Takato Odagiri,[4] Masato Tashiro,[4] Hirofumi Sawa,[5] Joe Chiba,[2] Takeshi Kurata,[1] Tetsutaro Sata,[1] and Hideki Hasegawa[1*]

[1]Department of Pathology, National Institute of Infectious Diseases, Gakuen, Musashimurayama-shi, Tokyo, Japan
[2]Department of Biological Science and Technology, Tokyo University of Science, Yamazaki, Noda, Chiba, Japan
[3]CMP Therapeutics Ltd., Oxford, UK
[4]Department of Virology III, National Institute of Infectious Diseases, Gakuen, Musashimurayama-shi, Tokyo, Japan
[5]Department of Molecular Pathobiology, 21st Century COE Program for Zoonosis Control, Hokkaido University Research Center for Zoonosis Control, Kita-ku, Sapporo, Japan

Highly pathogenic avian influenza virus (H5N1) is an emerging pathogen with the potential to cause great harm to humans, and there is concern about the potential for a new influenza pandemic. This virus is resistant to the antiviral effects of interferons and tumor necrosis factor-α. However, the mechanism of interferon-independent protective innate immunity is not well understood. The prophylactic effects of chitin microparticles as a stimulator of innate mucosal immunity against a recently obtained strain of H5N1 influenza virus infection were examined in mice. Clinical parameters and the survival rate of mice treated by intranasal application of chitin microparticles were significantly improved compared to non-treated mice after a lethal influenza virus challenge. Flow cytometric analysis revealed that the number of natural killer cells that expressed tumor necrosis factor-related apoptosis-inducing ligand (TRAIL) and that had migrated into the cervical lymph node was markedly increased (26-fold) after intranasal treatment with chitin microparticles. In addition, the level of IL-6 and interferon-gamma-inducible protein-10 (IP-10) in the nasal mucosa after H5N1 influenza virus challenge was decreased by prophylactic treatment with chitin microparticles. These results suggest that prophylactic intranasal administration of chitin microparticles enhanced the local accumulation of natural killer cells and suppressed hyper-induction of cytokines, resulting in an innate immune response to prevent pathogenesis of H5N1 influenza virus. ***J. Med. Virol. 79:811–819, 2007.***

KEY WORDS: influenza virus H5N1; innate immunity; chitin

INTRODUCTION

Avian influenza A subtype H5N1 outbreaks involving fatal human respiratory disease were reported in Hong Kong in 1997 (H5N1/97) [Claas et al., 1998; Subbarao et al., 1998]. The subsequent re-emergence of human H5N1 disease with high fatality rates has been reported in southern China [Peiris et al., 2004], Vietnam [Tran et al., 2004], Thailand [Grose and Chokephaibulkit, 2004], Cambodia, Indonesia, Turkey, and Iraq. At least 278 laboratory-confirmed cases of human infection with a fatality rate of greater than 50% were reported to the World Health Organization [2007] from January 2003 to March 2007. It has been reported that an oseltamivir-resistant H5N1 influenza virus (A/Hanoi/30408/2005) was isolated from a Vietnamese girl [Le et al., 2005], and H5N1 influenza viruses isolated from Hong Kong (A/Hong Kong/156/97, A/Hong Kong/483/97, and A/Hong Kong/486/97) were resistant to the antiviral effects of interferons and tumor necrosis factor-α [Seo et al., 2002].

Natural killer cells eliminate tumor cells and cells infected by viruses, including influenza virus, via their cytotoxic activity and production of cytokines [Biron and Brossay, 2001; Cooper et al., 2001; Gazit et al., 2006]. Natural killer cells are rapidly recruited to sites of infection, and can inhibit viral replication and dissemination through the respiratory tract

†Research Fellow of the Japanese Society for the Promotion of Science.

*Correspondence to: Hideki Hasegawa, Department of Pathology, National Institute of Infectious Diseases 4-7-1 Gakuen, Musashimurayama-shi, Tokyo 208-0011, Japan.
E-mail: hasegawa@nih.go.jp

Accepted 5 February 2007
DOI 10.1002/jmv.20837
Published online in Wiley InterScience (www.interscience.wiley.com)

[Stein-Streilein et al., 1983; Stein-Streilein and Guffee, 1986, and unpublished data by P. Strong]. Thus, natural killer cells play a role in the early stage of host defense against viral infection, and also bridge the subsequent adaptive anti-viral immune responses [Kos and Engleman, 1996; Biron, 1997; Biron et al., 1999; Andoniou et al., 2005; O'Leary et al., 2006]. Although the precise mechanism of the innate immune response to highly pathogenic H5N1 influenza virus is still unknown, the role of natural killer cells in innate immunity against viral infection seems to be important.

Chitin (a natural polysaccharide of *N*-acetyl-D-glucosamine), one of the most abundant polysaccharides in nature, is an essential component of fungal walls and the exoskeletons of crabs, shrimp, and insects. Chitin is non-allergenic, non-toxic, bio-degradable and biocompatible. Chitin-derived products are now widely used in the medical, veterinary, cosmetic, health supplement, and environmental industries [Okamoto et al., 1993]. Chitosan, a highly deacetylated form of chitin, has been used as a vaccine adjuvant due to its muco-adhesive properties, and has been shown to enhance antibody responses to mucosally delivered vaccine antigens [Bacon et al., 2000]. Chitin microparticles (1–20 μm in diameter), in contrast to chitosan, have strong immunomodulatory properties. Previous studies showed that chitin microparticles had effective adjuvant activity with an inactivated influenza vaccine [Hasegawa et al., 2005] or with an HIV-DNA vaccine [Hamajima et al., 2003]. Chitin microparticles, when administered intranasally, have also been found to reduce symptoms of respiratory allergy and allergic asthma [Strong et al., 2002; Ozdemir et al., 2006]. Other studies using chitin microparticles have demonstrated their Th1-inducing properties and shown that phagocytosis of chitin microparticles by macrophages through involves the mannose receptor and results in the production of IL-12, IL-18, and tumor necrosis factor-α, which in turn stimulated natural killer cells to produce IFN-γ [Shibata et al., 1997a,b, 1998].

In the present study, prophylactic use of intranasally applied chitin microparticles to stimulate innate mucosal immunity to lethal H5N1 influenza virus challenge is investigated. It is shown that intranasal pretreatment with chitin microparticles induces expression of tumor necrosis factor-related apoptosis-inducing ligand (TRAIL) in a large proportion of natural killer cells in the cervical lymph node, and suppresses viral load and hyper-induction of cytokines that may play a role in the pathogenesis of H5N1 [Chan et al., 2005; de Jong et al., 2006].

MATERIALS AND METHODS

Mice

Six- to 8-week-old female BALB/c mice were purchased from Japan SLC. Mice were kept under specific-pathogen-free conditions approved by the Institution Animal Care and Use Committee of National Institute of Infectious Diseases.

Viruses

The mouse-adapted strains of A/Puerto Rico/8/34 (A/PR8, H1N1) and wild-type A/Vietnam/1194/04 (VN1194, H5N1) viruses were used in this study. The A/PR8 virus was passaged 148 times in the ferret, 596 times in the mouse, and 73 times in 10-day fertile chicken eggs. The VN1194 virus isolated from patients with H5N1 disease in Vietnam in 2004 was prepared in Mardin-Darby canine kidney (MDCK) cells without any additional special steps for mouse adaptation. These viruses were stored at −80°C and viral titers were quantified by plaque assay.

Preparation of Chitin Microparticles, Poly(I:C) and LPS

Chitin microparticles prepared from shrimp derived chitin was kindly provided by P. Strong (CMP Therapeutics Ltd., Oxford, UK). Particle size was determined by Christison Particle Technologies (Gateshead, UK) using a Model 780 Accusizer and the average particle size was 10 μm. The sterility of the chitin microparticles was confirmed by plating on agar plates. The concentration of endotoxin in the chitin microparticles preparations was examined by Limulus Amebocyte Lysate Assay (BioWhittaker, Wokingham, UK) and shown to be less than 1 EU/ml. Synthetic dsRNA [poly(I:C)] was kindly provided by Toray Industries, Inc. (Kamakura, Kanagawa, Japan). Lipopolysaccharide (LPS) was purchased from Sigma (St. Louis, MO).

Pretreatment with Chitin Microparticles, Poly(I:C) and LPS and Virus Infection in Mice

To assess the efficacy of intranasal pretreatment with innate immune stimulators as prophylactic agents against influenza (A/PR8, H1N1) and highly pathogenic avian influenza (VN1194, H5N1) strains, chitin microparticles (100 μg), poly(I:C) (10 μg), LPS (1 μg) or PBS were administered intranasally to mice. CMP treatments were performed once a day for 2 or 3 days and other treatments were performed once (6 hr) before viral challenge. Previous experiments established the optimum dosing schedule for CMP, poly(I:C), and LPS. These amounts of each of the innate stimulators were sufficient to generate adjuvant activity against influenza virus infection when they were administered intranasally with vaccine [Ichinohe et al., 2005, 2006]. Five mice for each experimental group were anesthetized with diethyl ether and received an intranasal application of 10 μl of PBS containing chitin microparticles, poly(I:C) or LPS (5 μl/each nostril) prior to influenza virus infection. Mice were anesthetized 6 hr after final administration, and 2 μl of a suspension of influenza virus (A/PR8 or VN1194) was dropped into each nostril (4 μl per mouse). Virus titers of nasal washes were measured 3 days after inoculation of the influenza virus. H5N1 virus infection experiments were carried out in biosafety level 3 containment facilities approved

by the Guides for Animal Experiments Performed at the National Institute of Infectious Diseases.

Titration of Virus

Mice were given 100 μg of chitin microparticles or PBS twice intranasally at 30 and 6 hr before infection, then infected with 1,000 PFU of H5N1 influenza virus. Mice (n = 3 mice per time point) were sacrificed and tissues were collected 3, 5, 8, or 10 days post-infection. Viral titration in the frontal lobe, trigeminal nerve ganglia, brain stem, cervical lymph node, spleen, liver, kidney, large intestine, muscle, serum, nasal wash, and lung wash of infected mice was determined by plaque assay using MDCK cells (Fig. 4). Lung washes and nasal washes were prepared in PBS containing 0.1% bovine serum albumin, as described previously [Asahi et al., 2002] and used for viral titration after removing cellular debris by centrifugation. Tissue homogenates (1–10%, w/v) were prepared in PBS containing 0.1% bovine serum albumin, centrifuged at 9,170*g* for 10 min, and supernatants were inoculated into cells in the presence of 10 μg/ml acetylated trypsin (Sigma).

Flow Cytometry

Mice were given 100 μg of chitin microparticles intranasally once a day for 3 days, and sacrificed 6 hr after the final administration to collect the cervical lymph node. The number of natural killer cells in the local lymphoid tissue was analyzed by three-color flow cytometry. Single cell suspensions were prepared from the cervical lymph node and red blood cells were depleted by incubation in 0.83% NH_4Cl. Cells were incubated with 5 μg/ml of anti-mouse CD16/32 antibody (eBioscience, San Diego, CA) to block nonspecific binding, then incubated with FITC-labeled anti-mouse pan-natural killer cell antibody (Dx5, eBioscience) and phycoerythrin (PE)-labeled anti-mouse tumor necrosis factor-related apoptosis-inducing ligand (TRAIL) antibody (N2B2, eBioscience). To quantitate the total number of live cells an aliquot of cells were incubated with propidium iodide (PI, final concentration; 5 μg/ml). Samples were analyzed with a flow cytometer (FACS-Calibur, BD Biosciences, San Jose, CA), and the data were analyzed with CELLQuest software.

Multiplex Cytokine Assays

Mice were given 100 μg of chitin microparticles or PBS intranasally once a day for 2 days, then infected with 1,000 PFU of H5N1 influenza virus. After the challenge, mice were sacrificed to collect nasal washes at 3, 5, 8, or 10 days post-infection. Samples of nasal washes were analyzed for 20 cytokines (FGF basic, GM-CSF, IFN-γ, IL-1α, IL-1β, IL-2, IL-4, IL-5, IL-6, IL-10, IL-12, IL-13, IL-17, IP-10, KC, MCP-1, MIG, MIP-1α, TNF-α, and VEGF) by Luminex 200™ (Luminex Co., Austin, TX) using mouse cytokine twenty-plex antibody bead kit (BioSource International, Inc. Camarillo, CA), according to the manufacturer's instructions. Briefly, Multiplex beads were vortexed and sonicated for 30 s and 25 μl of beads suspension was added to each well of a 96 well filter plate and washed twice with wash buffer. The nasal wash were diluted 1:1 in assay diluent and loaded onto a Millipore Multiscreen BV 96-well filter plate to which 50 μl of incubation buffer had been added to each well. Serial dilutions of cytokines standards were prepared in parallel and added to the plate. Samples were incubated on a plate shaker in the dark at room temperature for 2 hr. The plate was applied to a Millipore Multiscreen Vacuum Manifold, washed twice with 200 μl wash buffer, and 100 μl of biotinylated Anti-Mouse Multi-Cytokine Detector Antibody was added to each well. The plate was shaken again as above for 1 hr applied to a Millipore Multiscreen Vacuum Manifold, and washed twice with 200 μl wash buffer. One hundred microliters of Streptavidin R-phycoerythrin was added directly to each well, plate was shaken again as above for 30 min, applied to the vacuum manifold, and washed twice. One hundred microliters of wash buffer was added to each well and the plate was shaken for 3 min. The assay plate was analyzed using the Bio-Plex Luminex 100 XYP instrument. Cytokine concentrations were calculated using Bio-Plex Manager 3.0 software with a five parameter curve-fitting algorithm applied for standard curve calculation.

Statistics

Comparisons between experimental groups were made using the Student's *t*-test for paired observations; $P < 0.05$ was considered statistically significant.

RESULTS

Protective Effect of Chitin Microparticles on A/PR8 (H1N1) or A/Vietnam (H5N1) Influenza virus Infection

To assess the efficacy of intranasal pretreatment with chitin microparticles as a prophylactic treatment against avirulent (A/PuertoRico/8/34/, H1N1) or highly pathogenic avian influenza virus infection (A/Vietnam/1194/2004, H5N1), a chitin microparticle suspension was given intranasally to mice. After H1N1 viral challenge, mice pretreated intranasally with either poly(I:C) or LPS given 6 hr prior to infection showed a marked reduction in virus titer in their nasal wash (Fig. 1A). Mice treated with three daily doses of CMP showed a partial but significant reduction of nasal-wash virus titers (Fig. 1A). The protective effect of chitin microparticles against H5N1 influenza virus infection was also examined. Mice treated intranasally with three daily doses of chitin microparticles showed a marked reduction in virus titer in their nasal washes, although mice pretreated with either poly(I:C) or LPS showed only a partial reduction in virus titers in their nasal

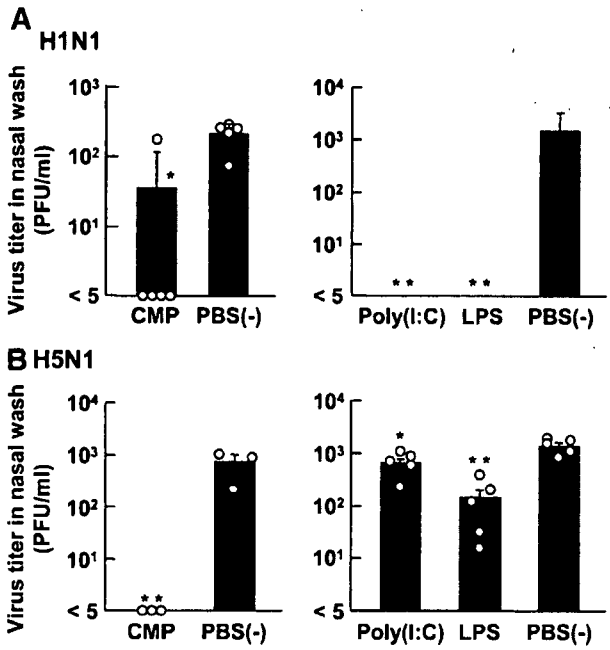

Fig. 1. Protective effect of innate immune stimulators against H1N1 and H5N1 influenza virus infection in BALB/c mice. A: Mice (n = 5 mice per group) received 100 μg of chitin microparticles (CMP) once a day for 3 days, or 10 μg of poly(I:C), 1 μg of LPS, or PBS once 6 hr before viral challenge, then were infected intranasally with 100 PFU of A/PR8 (H1N1) influenza viruses in 2 μl suspension for each nostril. Virus titers in nasal washes 3 days post-inoculation are shown. B: Mice were pretreated as above and infected intranasally with 1,000 PFU of VN1194 (H5N1) influenza viruses in 2 μl suspension for each nostril. Virus titers in nasal washes 3 days post-inoculation are shown. Data represents the means ± standard error (SE). Open circles indicate values for individual mice. Asterisks indicate significant differences compared with infected controls: $^{*}P < 0.05$; $^{**}P < 0.01$.

washes (Fig. 1B). These results suggest that chitin microparticles can stimulate an immunological reaction that leads to reduction of viral replication in vivo.

Pretreatment With Chitin Microparticles Protects Mice From Lethal Infection of H1N1 and H5N1

The mortality of mice after inoculation with a lethal dose of H1N1 or H5N1 influenza virus was monitored. Chitin microparticles (100 μg) was given intranasally once a day for 3 days before infection with 100 PFU (4 LD50) of H1N1 virus in a 20 μl suspension (Fig. 2A,B). All the control mice pre-treated with PBS were dead 9 days after infection, with marked clinical symptoms of disease and marked reduction of body weight. Mice pretreated with chitin microparticles also lost weight and developed clinical symptoms, but 15 days after infection, 60% of mice recovered their body weight, and survived for the duration of the experiment (at least 40 days after infection).

The prophylactic effect of chitin microparticles against lethal H5N1 influenza virus infection was also examined. Mice were given 100 μg of chitin microparticles intranasally once a day for 2 days, or PBS 6 hr

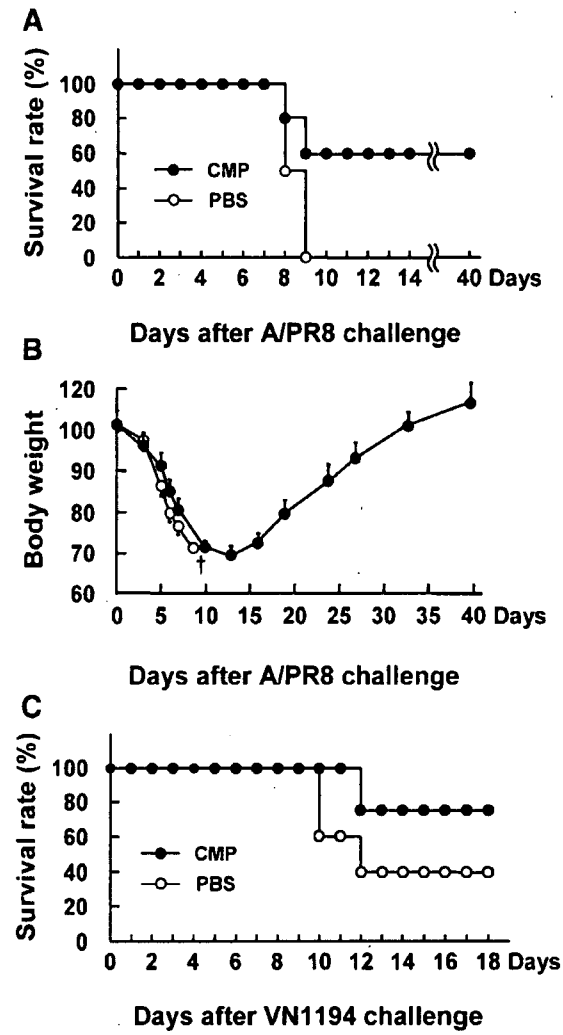

Fig. 2. Prophylactic effect of chitin microparticles (CMP) against H1N1-induced pneumonia or H5N1 influenza virus infection. Mice (n = 4–5 mice per group) were administered 100 μg of chitin microparticles to the lung intranasally in a volume of 20 μl PBS once a day for 3 days (closed circles) or PBS (open circles), then challenged with a lethal dose (4 LD50) of A/PR8/H1N1 influenza virus in 20 μl PBS to the lung. Survival curves (A) and body weight changes over time (B) after virus challenge are shown. Body weights are plotted as a percentage of the average initial weight. The open cross indicates the time-point at which all mice in a group succumbed to disease. Infected mice were monitored for 40 days. C: Mice (n = 5 mice per group) received 100 μg of chitin microparticles once a day for 2 days (closed circles), or PBS (open circles), then infected intranasally with 1,000 PFU of VN1194 (H5N1) influenza virus in 2 μl suspension for each nostril. Survival curves after virus challenge are shown. The survival rates were monitored for 18 days.

before intranasal infection with 1,000 PFU of H5N1 influenza viruses. Interestingly, intranasal administration of chitin microparticles led to a significant improvement in survival and fewer clinical symptoms compared with PBS-treated control mice (Fig. 2C). These results suggested that intranasal pretreatment with chitin microparticles protects mice against both H1N1 and H5N1 lethal infections.

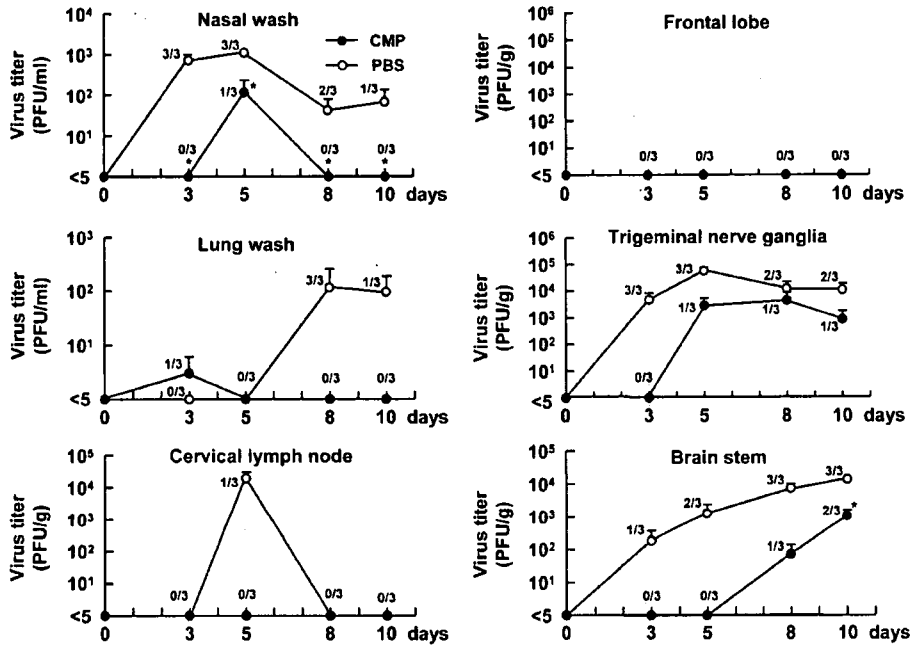

Fig. 3. Virus titers in various organs after challenge with 1,000 PFU of VN1194 (H5N1). Mice were administered 100 μg of chitin microparticles (CMP) intranasally once a day for 2 days (closed circle) or PBS (open circle), and infected with 1,000 PFU of VN1194 influenza virus. Mice were sacrificed to collect organs 3, 5, 8, or 10 days post-inoculation. Virus titers in the indicated organs after viral challenge are shown. Data represents the means ± SE, and represents the numbers of mice that failed to clear viruses/total number of mice (n = 3). Asterisks indicate significant differences compared to the PBS control group; $P < 0.05$.

Reduction of H5N1 Influenza Virus Titer in Multiple Organs by Pretreatment with Chitin Microparticles

To examine the efficiency of viral spread of A/Vietnam/1194/04 (H5N1) after nasal infection in mice, viral titers in multiple tissues from mice intranasally infected with 1,000 PFU of H5N1 were measured 3, 5, 8, and 10 days after infection with or without chitin microparticles pretreatment (n = 3 mice per time point). Mice were given 100 μg of chitin microparticles or PBS intranasally twice at 30 and 6 hr before infection, then infected with 1,000 PFU of H5N1 influenza viruses. When the mice were infected with a small volume (2 μl in each nostil) of virus suspension without chitin microparticles pretreatment, virus titers were detected in nasal washes and in the trigerminal nerve ganglia of all mice 3 days post-inoculation, and were highest at 5 days post-inoculation (open circles in Fig. 3). Thereafter, virus was detected in the lung and brain stem 8 days post-inoculation (open circles in Fig. 3). Interestingly, live virus was not detected in the frontal lobe of the cerebrum, which is directly connected to the nasal cavity via the olfactory nerve. No live virus was detected in the spleen, liver, kidney, large intestine, muscle, or serum of mice (data not shown).

In the nasal wash and brain stem of chitin microparticles-treated mice, the virus titer was significantly reduced compared to PBS-treated mice (closed circles in Fig. 3). In addition, virus titers tended to be much lower in lung washes, cervical lymph node, and terminal nerve ganglia in the chitin microparticles-treated group compared to the control group (closed circles in Fig. 3). Live virus titers were not detected in the frontal lobe of the cerebrum.

Migration of Natural Killer Cells Expressing Tumor Necrosis Factor-Related Apoptosis-Inducing Ligand (TRAIL) in the Cervical Lymph Node After Intranasal Administration of Chitin Microparticles

Previous work suggested that chitin microparticles given intranasally induced an accumulation of natural killer cells in local lymphoid tissue (unpublished data). To define the mechanism of the protective effect of chitin microparticles against highly pathogenic H5N1 influenza virus infection, the migration of natural killer cells into the cervical lymph node was examined. The proportion of natural killer cells in the cervical lymph node increased 6-fold in chitin microparticles-treated mice compared with PBS-treated mice 6 hr after chitin microparticles administration (Fig. 4A). As tumor necrosis factor-related apoptosis-inducing ligand (TRAIL) plays an important role in the immune response of natural killer cells to influenza virus infection [Ishikawa et al., 2005], the number of natural killer cells expressing tumor necrosis factor-related apoptosis-inducing ligand (TRAIL) on their cell surface was counted. The number of tumor necrosis factor-

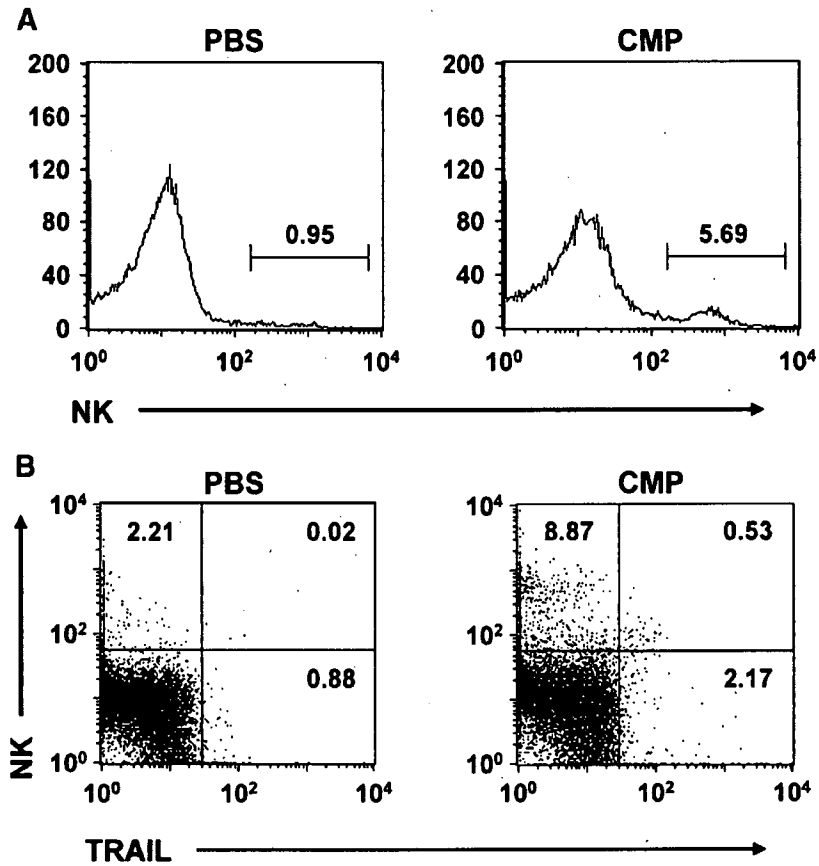

Fig. 4. Increased natural killer (NK) cell migration into the cervical lymph node after intranasal chitin microparticles (CMP) treatment. Mice were administered 100 μg of chitin microparticles intranasally once a day for 3 days or PBS, and sacrificed to collect the cervical lymph node 6 hr after the final administration. cervical lymph node cells of 5 mice were pooled and stained with PI and anti-mouse CD49bFITC and/or anti-mouse tumor necrosis factor-related apoptosis-inducing ligand (TRAIL) PE antibodies. Viable cells (PI−) were selected with forward and side scatter gated for lymphocytes. The expression of CD49b and tumor necrosis factor-related apoptosis-inducing ligand (TRAIL) was analyzed in this population. A: Numbers in each histogram above the marker indicate the percentage of 'live'-gated cells deemed panCD49b+. B: CD49b and tumor necrosis factor-related apoptosis-inducing ligand (TRAIL) profile of cells recovered from the cervical lymph node of mice pretreated with chitin microparticles or PBS. Figure is representative of three experiments.

related apoptosis-inducing ligand (TRAIL)-expressing natural killer cells increased 26-fold in the cervical lymph node of chitin microparticles treated mice compared with PBS-treated mice (Fig. 4B). These results suggest that migration of natural killer cells expressing tumor necrosis factor-related apoptosis-inducing ligand (TRAIL) into local lymph nodes might play a role in the reduction of virus titer and improvement of clinical symptoms in virus infected mice.

Reduction of IL-6 and Interferon-Gamma-Inducible Protein-10 (IP-10) Secretion From Nasal Mucosa by Pretreatment with Chitin Microparticles in H5N1 Influenza Virus Infection

Chitin microparticles might also play a role in the reduction of inflammatory cytokines and chemokines that accompany H5N1 influenza virus infection. To examine this possibility, the level of secreted cytokines described in the Materials and Methods in nasal mucosa was examined in mice infected with H5N1 virus with or without chitin microparticles pretreatment. Among them the secretion of IL-6 in nasal mucosa was up-regulated by H5N1 influenza virus infection 10 days post-inoculation, while in the chitin microparticles-treated group, there was a marked reduction of IL-6 secretion (Fig. 5A). Likewise, the secretion of interferon-gamma-inducible protein-10 (IP-10) was inhibited in mice pretreated with chitin microparticles compared to the PBS-treated group 8 days post-inoculation (Fig. 5B). On the other hand tumor necrosis factor-α was not detected in nasal mucosa of mice after H5N1 influenza virus infection (data not shown). These results suggested that chitin microparticles pretreatment may inhibit the hyper-induction induction of cytokines and chemokines that are relevant to the pathogenesis of H5N1 influenza virus in infected mice.

DISCUSSION

The present study demonstrated that intranasal administration of a suspension of chitin microparticles

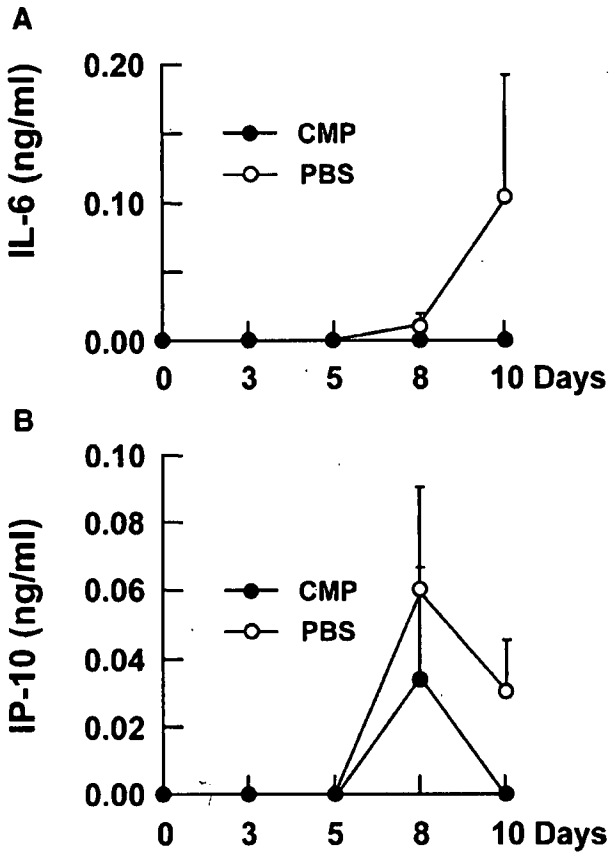

Fig. 5. Kinetics of IL-6 (A) and interferon-gamma-inducible protein-10 (IP-10) (B) secretion in the nasal mucosa after H5N1 influenza virus infection. Mice (n = 3) were administered 100 μg of chitin microparticles (CMP) intranasally once a day for 2 days (closed circles) or PBS (open circles), then infected with 1,000 PFU of VN1194 (H5N1) influenza virus. After viral challenge, mice were sacrificed to collect nasal washes 3, 5, 8, or 10 days post-inoculation. The levels of each cytokine in nasal washes after the viral challenge are shown. Data represents the means ± SE.

has protective effects against lethal H5N1 influenza virus infection of the upper respiratory tract in mice. These findings were consistent with results showing the protective effects against avirulent influenza virus (A/PR8, H1N1) infection in mice by intranasal administration of chitin microparticles into the lung (unpublished data by P. Strong). It is previously reported that chitin microparticles had a mucosal adjuvant effect when co-administered with an influenza hemagglutinin vaccine and increased both the mucosal and systemic humoral responses that provided complete protection against challenge with the homologous influenza virus H1N1 or H5N1 in mice [Hasegawa et al., 2005; Asahi-Ozaki et al., 2006; Ichinohe et al., 2006]. The current study demonstrates hitherto unrecognized effects of chitin microparticles in enhancing innate protection against infection with a highly pathogenic avian influenza virus strain.

It has been reported that the highly pathogenic H5N1 influenza virus induces high levels of pro-inflammatory cytokines and chemokines that may play a role in the pathogenesis of [Chan et al., 2005; de Jong et al., 2006]. It is demonstrated that intranasal administration of chitin microparticles induced the accumulation of natural killer cells expressing tumor necrosis factor-related apoptosis-inducing ligand (TRAIL) in the cervical lymph node and suppressed viral load and hyper-induction of cytokines. These results suggested that recruitment of natural killer cells expressing tumor necrosis factor-related apoptosis-inducing ligand (TRAIL) into local sites of infection (Fig. 4) and suppression of pro-inflammatory cytokines and chemokines (e.g. IL-6 and interferon-gamma-inducible protein-10 in Fig. 5) may contribute to a reduction of clinical symptoms and enhance protection against lethal H5N1 influenza virus infection.

The importance of natural killer cells in viral defense has been demonstrated most convincingly in a patient who lacked natural killer cells and was therefore susceptible to virus infections [Biron et al., 1989]. Mice in which natural killer cells have been depleted demonstrated increased mortality after infection with influenza viruses [Stein-Streilein and Guffee, 1986]. Therefore, it might be expected that the enhancement of natural killer cells activity by chitin microparticles and the accumulation of natural killer cells locally into the site of infection and an enhancement of tumor necrosis factor-related apoptosis-inducing ligand (TRAIL) expression on their surface (Fig. 4) might increase resistance to viral infection. In natural killer cells or T-cells, tumor necrosis factor-related apoptosis-inducing ligand (TRAIL) plays an important role in the immune response to influenza virus infection [Ishikawa et al., 2005]. Presumably due to this recruitment of tumor necrosis factor-related apoptosis-inducing ligand (TRAIL)-expressing natural killer cells, H5N1 virus titers were suppressed in nasal washes, lung washes, cervical lymph node, trigeminal nerve ganglia and in the brain stem of mice pretreated with chitin microparticles compared to mice in the control group (Fig. 3). Consistent with these findings, pretreatment of mice with chitin microparticles led to a significant improvement in survival rate and reduction in clinical symptoms following H5N1 virus infection (Fig. 2A,B) and H1N1 virus infection (Fig. 2C).

Finally, the present studies suggest that intranasal administration of chitin microparticles boosts innate immunity and protects mice from infection by the highly pathogenic H5N1 influenza virus infection in the upper respiratory tracts. It is proposed that if mice are given chitin microparticles as a daily prophylactic they would have enhanced protection against infection with H5N1. This prophylactic effect is elicited by activation of natural killer cells and regulation of inflammatory cytokines such as IL-6 and interferon-gamma-inducible protein-10 (IP-10). The adjuvant effects of chitin microparticles are also expected [Hasegawa et al., 2005; Asahi-Ozaki et al., 2006; Ichinohe et al., 2006] in inducing adaptive immunity following infection. Identification of therapeutic innate immunity enhancing agents such as chitin microparticles may lead to

antiviral strategies against the highly pathogenic H5N1 influenza virus and may have relevance as part of a first line defense against H5N1 outbreaks.

ACKNOWLEDGMENTS

We are grateful to Dr. Wilina Lim (Department of Health, The government of Hong Kong) for providing us A/Vietnam/1194/04 (H5N1) influenza virus strain, and Dr. U. Suzuki and Dr. K. Komase (Kitasato Institute, Saitama) and Dr. T. Tanaka (Toray Industries, Inc.) for providing the materials and Dr. M. Moriyama for helpful discussion. This work was supported in part by grants from the Ministry of Health, Labor, and Welfare, and Research on Health Sciences focusing on Drug Innovation.

REFERENCES

Andoniou CE, van Dommelen SL, Voigt V, Andrews DM, Brizard G, Asselin-Paturel C, Delale T, Stacey KJ, Trinchieri G, Degli-Esposti MA. 2005. Interaction between conventional dendritic cells and natural killer cells is integral to the activation of effective antiviral immunity. Nat Immunol 6:1011–1019.

Asahi Y, Yoshikawa T, Watanabe I, Iwasaki T, Hasegawa H, Sato Y, Shimada S, Nanno M, Matsuoka Y, Ohwaki M, Iwakura Y, Suzuki Y, Aizawa C, Sata T, Kurata T, Tamura S. 2002. Protection against influenza virus infection in polymeric Ig receptor knockout mice immunized intranasally with adjuvant-combined vaccines. J Immunol 168:2930–2938.

Asahi-Ozaki Y, Itamura S, Ichinohe T, Strong P, Tamura S, Takahashi H, Sawa H, Moriyama M, Tashiro M, Sata T, Kurata T, Hasegawa H. 2006. Intranasal administration of adjuvant-combined recombinant influenza virus HA vaccine protects mice from the lethal H5N1 virus infection. Microbes Infect 8:2706–2714.

Bacon A, Makin J, Sizer PJ, Jabbal-Gill I, Hinchcliffe M, Illum L, Chatfield S, Roberts M. 2000. Carbohydrate biopolymers enhance antibody responses to mucosally delivered vaccine antigens. Infect Immun 68:5764–5770.

Biron CA. 1997. Activation and function of natural killer cell responses during viral infections. Curr Opin Immunol 9:24–34.

Biron CA, Brossay L. 2001. NK cells and NKT cells in innate defense against viral infections. Curr Opin Immunol 13:458–464.

Biron CA, Byron KS, Sullivan JL. 1989. Severe herpesvirus infections in an adolescent without natural killer cells. N Engl J Med 320: 1731–1735.

Biron CA, Nguyen KB, Pien GC, Cousens LP, Salazar-Mather TP. 1999. Natural killer cells in antiviral defense: function and regulation by innate cytokines. Annu Rev Immunol 17:189–220.

Chan MC, Cheung CY, Chui WH, Tsao SW, Nicholls JM, Chan YO, Chan RW, Long HT, Poon LL, Guan Y, Peiris JS. 2005. Proinflammatory cytokine responses induced by influenza A (H5N1) viruses in primary human alveolar and bronchial epithelial cells. Respir Res 6:135.

Claas EC, Osterhaus AD, van Beek R, De Jong JC, Rimmelzwaan GF, Senne DA, Krauss S, Shortridge KF, Webster RG. 1998. Human influenza A H5N1 virus related to a highly pathogenic avian influenza virus. Lancet 351:472–477.

Cooper MA, Fehniger TA, Caligiuri MA. 2001. The biology of human natural killer-cell subsets. Trends Immunol 22:633–640.

de Jong MD, Simmons CP, Thanh TT, Hien VM, Smith GJ, Chau TN, Hoang DM, Van Vinh Chau N, Khanh TH, Dong VC, Qui PT, Van Cam B, Ha do Q, Guan Y, Peiris JS, Chinh NT, Hien TT, Farrar J. 2006. Fatal outcome of human influenza A (H5N1) is associated with high viral load and hypercytokinemia. Nat Med 12:1203–1207.

Gazit R, Gruda R, Elboim M, Arnon TI, Katz G, Achdout H, Hanna J, Qimron U, Landau G, Greenbaum E, Zakay-Rones Z, Porgador A, Mandelboim O. 2006. Lethal influenza infection in the absence of the natural killer cell receptor gene Ncr1. Nat Immunol 7:517–523.

Grose C, Chokephaibulkit K. 2004. Avian influenza virus infection of children in Vietnam and Thailand. Pediatr Infect Dis J 23: 793–794.

Hamajima K, Kojima Y, Matsui K, Toda Y, Jounai N, Ozaki T, Xin KQ, Strong P, Okuda K. 2003. Chitin micro-particles (CMP): a useful adjuvant for inducing viral specific immunity when delivered intranasally with an HIV-DNA vaccine. Viral Immunol 16:541–547.

Hasegawa H, Ichinohe T, Strong P, Watanabe I, Ito S, Tamura S, Takahashi H, Sawa H, Chiba J, Kurata T, Sata T. 2005. Protection against influenza virus infection by intranasal administration of hemagglutinin vaccine with chitin microparticles as an adjuvant. J Med Virol 75:130–136.

Ichinohe T, Watanabe I, Ito S, Fujii H, Moriyama M, Tamura S, Takahashi H, Sawa H, Chiba J, Kurata T, Sata T, Hasegawa H. 2005. Synthetic double-stranded RNA poly(I:C) combined with mucosal vaccine protects against influenza virus infection. J Virol 79:2910–2919.

Ichinohe T, Watanabe I, Tao E, Ito S, Kawaguchi A, Tamura S, Takahashi H, Sawa H, Moriyama M, Chiba J, Komase K, Suzuki Y, Kurata T, Sata T, Hasegawa H. 2006. Protection against influenza virus infection by intranasal vaccine with surf clam microparticles (SMP) as an adjuvant. J Med Virol 78:954–963.

Ishikawa E, Nakazawa M, Yoshinari M, Minami M. 2005. Role of tumor necrosis factor-related apoptosis-inducing ligand in immune response to influenza virus infection in mice. J Virol 79:7658–7663.

Kos FJ, Engleman EG. 1996. Role of natural killer cells in the generation of influenza virus-specific cytotoxic T cells. Cell Immunol 173:1–6.

Le QM, Kiso M, Someya K, Sakai YT, Nguyen TH, Nguyen KH, Pham ND, Ngyen HH, Yamada S, Muramoto Y, Horimoto T, Takada A, Goto H, Suzuki T, Suzuki Y, Kawaoka Y. 2005. Avian flu: isolation of drug-resistant H5N1 virus. Nature 437:1108.

Okamoto Y, Minami S, Matsuhashi A, Sashiwa H, Saimoto H, Shigemasa Y, Tanigawa T, Tanaka Y, Tokura S. 1993. Application of polymeric *N*-acetyl-D-glucosamine (chitin) to veterinary practice. J Vet Med Sci 55:743–747.

O'Leary JG, Goodarzi M, Drayton DL, von Andrian UH. 2006. T cell- and B cell-independent adaptive immunity mediated by natural killer cells. Nat Immunol 7:507–516.

Ozdemir C, Yazi D, Aydogan M, Akkoc T, Bahceciler NN, Strong P, Barlan IB. 2006. Treatment with chitin microparticles is protective against lung histopathology in a murine asthma model. Clin Exp Allergy 36:960–968.

Peiris JS, Yu WC, Leung CW, Cheung CY, Ng WF, Nicholls JM, Ng TK, Chan KH, Lai ST, Lim WL, Yuen KY, Guan Y. 2004. Re-emergence of fatal human influenza A subtype H5N1 disease. Lancet 363:617–619.

Seo SH, Hoffmann E, Webster RG. 2002. Lethal H5N1 influenza viruses escape host anti-viral cytokine responses. Nat Med 8:950–954.

Shibata Y, Foster LA, Kurimoto M, Okamura H, Nakamura RM, Kawajiri K, Justice JP, Van Scott MR, Myrvik QN, Metzger WJ. 1998. Immunoregulatory roles of IL-10 in innate immunity: IL-10 inhibits macrophage production of IFN-gamma-inducing factors but enhances NK cell production of IFN-gamma. J Immunol 161:4283–4288.

Shibata Y, Foster LA, Metzger WJ, Myrvik QN. 1997a. Alveolar macrophage priming by intravenous administration of chitin particles, polymers of *N*-acetyl-D-glucosamine, in mice. Infect Immun 65:1734–1741.

Shibata Y, Metzger WJ, Myrvik QN. 1997b. Chitin particle-induced cell-mediated immunity is inhibited by soluble mannan: mannose receptor-mediated phagocytosis initiates IL-12 production. J Immunol 159:2462–2467.

Stein-Streilein J, Bennett M, Mann D, Kumar V. 1983. Natural killer cells in mouse lung: surface phenotype, target preference, and response to local influenza virus infection. J Immunol 131:2699–2704.

Stein-Streilein J, Guffee J. 1986. In vivo treatment of mice and hamsters with antibodies to asialo GM1 increases morbidity and mortality to pulmonary influenza infection. J Immunol 136:1435–1441.

Strong P, Clark H, Reid K. 2002. Intranasal application of chitin microparticles down-regulates symptoms of allergic hypersensitivity to *Dermatophagoides pteronyssinus* and *Aspergillus fumigatus* in murine models of allergy. Clin Exp Allergy 32:1794–1800.

Subbarao K, Klimov A, Katz J, Regnery H, Lim W, Hall H, Perdue M, Swayne D, Bender C, Huang J, Hemphill M, Rowe T, Shaw M, Xu X, Fukuda K, Cox N. 1998. Characterization of an avian influenza A

(H5N1) virus isolated from a child with a fatal respiratory illness. Science 279:393–396.

Tran TH, Nguyen TL, Nguyen TD, Luong TS, Pham PM, Nguyen VC, Pham TS, Vo CD, Le TQ, Ngo TT, Dao BK, Le PP, Nguyen TT, Hoang TL, Cao VT, Le TG, Nguyen DT, Le HN, Nguyen KT, Le HS, Le VT, Christiane D, Tran TT, Menno de J, Schultsz C, Cheng P, Lim W, Horby P, Farrar J. 2004. Avian influenza A (H5N1) in 10 patients in Vietnam. N Engl J Med 350:1179–1188.

World Health Organization. 2007. Cumulative number of confirmed human cases of avian influenza A/(H5N1) reported to WHO. http://www.who.int/csr/disease/avian_influenza/country/cases_table_2007_03_12/en/index.html

Laboratory Investigation (2007) 1–10

Hypomethylation of CD30 CpG islands with aberrant JunB expression drives CD30 induction in Hodgkin lymphoma and anaplastic large cell lymphoma

Mariko Watanabe[1,*], Yuji Ogawa[1,*], Kinji Itoh[2], Tukasa Koiwa[3], Marshall E Kadin[4], Toshiki Watanabe[3], Isao Okayasu[5], Masaaki Higashihara[1] and Ryouichi Horie[1]

High expression of CD30 and JunB is the hallmark of malignant cells in Hodgkin lymphoma (HL) and anaplastic large cell lymphoma (ALCL). Ligand-independent signaling by CD30 induces JunB, which activates the CD30 promoter, stabilizing CD30 expression and supporting the survival of Hodgkin–Reed–Sternberg (H–RS) and ALCL cells. Here we show for the first time CpG islands encompassing 60 CpG dinucleotides, located in the core promoter, exon 1 and intron 1 of CD30 gene. Analysis of the methylation status of CD30 CpG islands in H–RS, ALCL and unrelated cell lines reveals an inverse relationship between the extent of CD30 CpG methylation and CD30 expression. CD30 CpG islands of H–RS and ALCL cell lines are rarely methylated. Methylation of the CD30 promoter decreases CD30 induction and JunB action on the demethylated CD30 promoter enhances CD30 induction. CD30 and JunB are strongly expressed in H–RS and ALCL cells, whereas they are not expressed in nonmalignant lymphocytes in which CD30 CpG islands are rarely methylated. We conclude that constitutive action of aberrantly expressed JunB on hypomethylated CD30 CpG islands of lymphocytes triggers CD30 induction and initiates activation of the JunB-CD30-JunB loop, essential to the pathogenesis of HL and ALCL.

Laboratory Investigation advance online publication, 29 October 2007; doi:10.1038/labinvest.3700696

KEYWORDS: CD30; CpG methylation; JunB; Hodgkin lymphoma; anaplastic large cell lymphoma

CD30 is a member of the tumor necrosis factor (TNF) receptor superfamily initially identified on the surface of Hodgkin and Reed–Sternberg (H–RS) cells of Hodgkin lymphoma (HL).[1–3] Immunohistochemical analysis of a large range of human tumors has shown that CD30 is overexpressed not only by H–RS cells, but also by a subset of diffuse large cell neoplasms with anaplastic features called anaplastic large cell lymphoma (ALCL).[4,5]

Overexpression of CD30 is a characteristic of H–RS and ALCL cells. Ligand-independent signals triggered by overexpressed CD30 induce activation of NF-κB and the extracellular signal-regulated kinase (ERK) 1/2 mitogen-activated protein kinase (MAPK) pathway, both of which contribute to tumorigenesis and maintenance of survival of H–RS and ALCL cells.[6–9]

Approximately 98% of H–RS cells are derived from B cells and the remaining 2% of H–RS cells appear to be derived from T cells.[10,11] Amplification of genomic DNA and complementary DNA (cDNA) derived from single H–RS cells indicates a germinal center B-cell origin of most H–RS cells. However, the origin of H–RS cells with T-cell phenotype and that of ALCL cells is entirely unknown. Despite lack of information about the cell origin in T-cell HL and ALCL with CD30 overexpression, it is assumed H–RS and ALCL cells are derived from normal lymphocytes, which lack CD30 expression at resting state. Consequently, understanding the mechanisms for constitutive overexpression of CD30 is important to understand the pathogenesis of HL and ALCL.

Cloning and characterization of the promoter region of the CD30 gene enabled us to demonstrate that the CD30

[1]Department of Hematology, School of Medicine, Kitasato University, Sagamihara, Kanagawa, Japan; [2]Department of Pathology, School of Medicine, Toho University, Ohta-ku, Tokyo, Japan; [3]Laboratory of Tumor Cell Biology, Department of Medical Genome Sciences, Graduate School of Frontier Sciences, The University of Tokyo, Minato-ku, Tokyo, Japan; [4]Department of Dermatology and Skin Surgery, Roger Williams Medical Center, Providence, RI, USA and [5]Department of Pathology, School of Medicine, Kitasato University, Sagamihara, Kanagawa, Japan
Correspondence: Dr R Horie, MD, PhD, Department of Hematology, School of Medicine, Kitasato University, 1-15-1 Kitasato, Sagamihara, Kanagawa 228-8555, Japan.
E-mail: rhorie@med.kitasato-u.ac.jp
*These authors contributed equally to this work.

Received 15 September 2007; accepted 12 October 2007; published online 29 October 2007

promoter is composed of a microsatellite sequence (MS) containing CCAT repeats and a core promoter with Sp-1-binding sites. The Sp-1 site at −45 to −39 within core promoter is responsible for basal promoter activity.[12,13] On the other hand, the CCAT motif repeated in the CD30 MS represses the core promoter activity of CD30. We found that action of JunB on the AP-1 site in the upstream region of the CD30 core promoter is responsible for strong activity of the CD30 promoter in H–RS and ALCL cells.[14] We also showed ligand-independent CD30-ERK-MAPK signals induce amplification of JunB, which acts on the CD30 promoter to stabilize overexpression of CD30 in H–RS and ALCL cells.[9]

Methylation of dinucleotide cytosine-guanosine motifs (CpG), especially in CpG islands located within promoter regions, is a common mechanism of gene regulation. Until now, there was no knowledge of the role of epigenetic regulation of CD30 gene expression. To learn about the role of epigenetic regulation in CD30 overexpression, we analyzed the CD30 gene and identified CpG islands encompassing 60 CpG dinucleotides (CD30 CpG islands) within the core promoter and exon 1 and intron 1 of the CD30 gene. We studied the contribution of the methylation status of CD30 CpG islands and JunB expression levels to CD30 overexpression in CD30-positive and -negative cell lines including H–RS cells, ALCL cells, as well as in normal lymphocytes and germinal center cells. We confirmed our findings in tissue sections of HL and ALCL and nonmalignant lymphoid tissues.

MATERIALS AND METHODS

Cell Cultures

K562, HEK293, Jurkat, HeLa, ML1, ML2, FL and A549 cell lines were obtained from the Japanese Cancer Research Resources Bank (Tokyo, Japan) and Fujisaki Cell Biology Center (Okayama, Japan). ALCL cell lines (SUDHL1 and Karpas299) and H–RS cell lines (L428, KMH2, HDLM2, L540 and HDMYZ) were purchased from the German Collection of Microorganisms and Cell Cultures (Braunschweig, Germany). Nonadherent cell lines were cultured in RPMI 1640 and adherent cells in Dulbecco's modified Eagle's medium (DMEM) with supplementation of recommended concentrations of fetal calf serum (FCS) and antibiotics. Normal lymphocytes were separated from peripheral blood of healthy volunteers by differential centrifugation through Lymphoprep (AXIS SHIELD PoC AS, Oslo, Norway). Cells were washed with phosphate-buffered saline (PBS(−)) before use.

Northern Blotting

Northern blot analysis was carried out essentially as described.[15] Briefly, 1 μg per lane of poly (A)-selected RNA was size-fractionated by 1% formalin agarose gel electrophoresis and subsequently blotted onto Hybond-C extra nitrocellulose membranes (Amersham Bioscience, Piscataway, NJ, USA). Filters were hybridized in 4 × SSC, 1 × Denhardts, 0.5% sodium dodecyl sulfate (SDS), 0.1 M NaPO4 (pH 7.0), 10% Dextran Na at 65°C with 1.0×10^6 cpm/ml of random prime-labeled probes. After washing to a final stringency of 0.2 × SSC and 0.1% SDS at 65°C, filters were exposed to XAR-5 films (Eastman Kodak, Rochester, NY, USA) at −80°C. RT–PCR-amplified fragments of human CD30 and human GAPDH were used as probes.

Immunohistochemistry

Cultured cells were immunostained with antibodies for CD30 and JunB, and fluorescence signals were detected using confocal microscopy. Cells were first washed three times with PSB (−). Cytospin samples were prepared using 5×10^4 cells and fixed with 100% methanol for 10 min at room temperature, then cells were washed three times in PBS (−). Samples were incubated with primary antibody at the concentration of 5 μg/ml at 4°C for overnight and washed with PBS (−) three times. After incubation with fluorescence-labeled secondary antibody for 30 min at 37°C, samples were washed three times in PBS (−) and covered with a Perma Fluloro antifade reagent (Therme Shandon. Co., Pittsburgh, PA, USA). Fluorescence signals were detected using confocal microscopy (Radience, 2000) (Bio-Rad Laboratories, Hercules, CA, USA). Antibodies used were as follows; anti-CD30 mouse monoclonal antibody (Ber-H2) (DAKO Kyoto, Japan) and anti-JunB mouse monoclonal antibody (C-11) (Sata Cruz Biotechnology, Inc., Santa Cruz, CA, USA).

Immunostaining of JunB and CD30 was performed on paraffin-embedded specimens of normal peripheral blood mononuclear cell (PBMC) and tonsil as well as lymph nodes affected with HL or ALCL. Prior to incubation of the anti-JunB antibody (C-11) or anti-CD30 antibody (Ber-H2), a heat-induced antigen retrieval was performed. Immunodetection was carried out with biotinylated goat anti-mouse IgG, followed by peroxidase-labeled streptavidine (DAKO). HISTOFINE™ kit (Nichirei, Tokyo, Japan) was used to detect the color reaction for peroxidase, according to the manufacturer's instructions.

Immunoblotting

Immunoblot analysis was carried out as described.[9] Antibodies used were as follows; anti-CD30 antibody (Ber-H2) (DAKO) and anti-α tubulin mouse monoclonal antibody (TU-02) (Santa Cruz). Alkaline phosphatase-conjugated secondary antibodies are as follows; anti-mouse IgG (H&L) antibody (Promega Madison, WI, USA) and anti-mouse IgM antibody (Santa Cruz).

CpG Methylation Analysis of Cell Lines

Methylation of the cytosine residue of the CpG site was analyzed by the bisulfite genomic sequencing method with slight modifications.[16] Briefly, genomic DNA of cell culture samples was extracted by SDS/proteinase K digestion,

followed by standard phenol–chloroform extraction and ethanol precipitation. Five μg of genomic DNA was used for bisulfite treatment. The DNA sample in 0.3 N NaOH was heat denatured at 75°C for 20 min, followed by incubation at 55°C for 4 h in 4.8 M $Na_2S_2O_5$ and 0.5 mM hydroquinone (both from Sigma, St Louis, MO, USA). The sample DNA was purified using the Wizard DNA Clean-Up system (Promega, Madison, WI, USA) and treated with 0.3 N NaOH at 37°C for 20 min. DNA was precipitated with ethanol and dissolved in 50 μl of H_2O, and 1/20 of this solution was subjected to PCR amplification using the AccuPrime *Taq* DNA Polymerase System (Invitrogen Graningen, Netherlands). PCR was conducted with a set of primers indicated in Figure 1c as follows: forward primer, 5′-TAAGGGTATGG GAGAAGGTTT-3′; reverse primer, 5′-CCTCCCACCTA TAAATACTAAC-3′(converted cytosine residues are written in bold letters). All primer sequences were devoid of CpG dinucleotides to avoid biased amplification of methylated alleles. The reaction condition was as follows: initial denature at 94°C for 2 min, 45 cycles of 94°C for 30 s, 55°C for 30 s, 68°C for 1 min and the final extension at 68°C for 7 min. Amplified and gel-purified PCR products were cloned into pGEM-T Easy vector (Promega), and nucleotide sequences of 10 or more clones were determined.

Bisulfite DNA Sequencing Analysis

For DNA sequencing, we used an ABI PRISM 377 DNA Sequencer (Applied Biosystems, Foster City, CA, USA) and DYEnamic ET Terminator Cycle Sequencing Kit (Amersham Bioscience, Piscataway, NJ, USA).

5-Azacytidine Treatment

For 5-azacytidine (5-AzaC) (Sigma) treatment, HDMYZ, Jurkat, ML1, FL and HEK293 were seeded at a density of 10^5 cells/ml, and were treated with the demethylating agent 5-AzaC at 1 or 2 μM for 72 h at 37°C in a 5% CO_2 humidified atmosphere. Then, 5-AzaC was removed and cells were cultured for 48 h.

Reverse Transcriptase-PCR Analysis

Total RNA from culture cells was extracted using the QIAzol Lysis Reagent (QIAGEN GmbH, Hilden, Germamy) according to the manufacturer's instruction. Each reaction mixture contained 2 μg total RNA, 50 pmol oligo (dT) primer and 200 U SuperScript II reverse transcriptase (Invitrogen) in a 20 μl cocktail. After denaturation of RNA at 70°C for 10 min, reaction mixtures were pre-incubated for 2 min at 42°C, then incubated at 42°C with reverse transcriptase for 50 min and finally denatured at 70°C for 15 min. PCR amplifications were performed using Takara Ex *Taq* DNA Polymerase System (Takara, Kyoto, Japan) according to the manufacturer's instruction. Each specific primers used were follows: CD30 forward, 5′-CAGCTGAGGAGTGGTGCGTCGG-3′; CD30 reverse, 5′-TCTGTCTCCTGCTCGGGGTAGTG-3′; β actin forward, 5′-TCAGAAGGACTCCTATGTGG-3′; β actin reverse, 5′-TCTCTTTGATGTCACGCACG-3′.

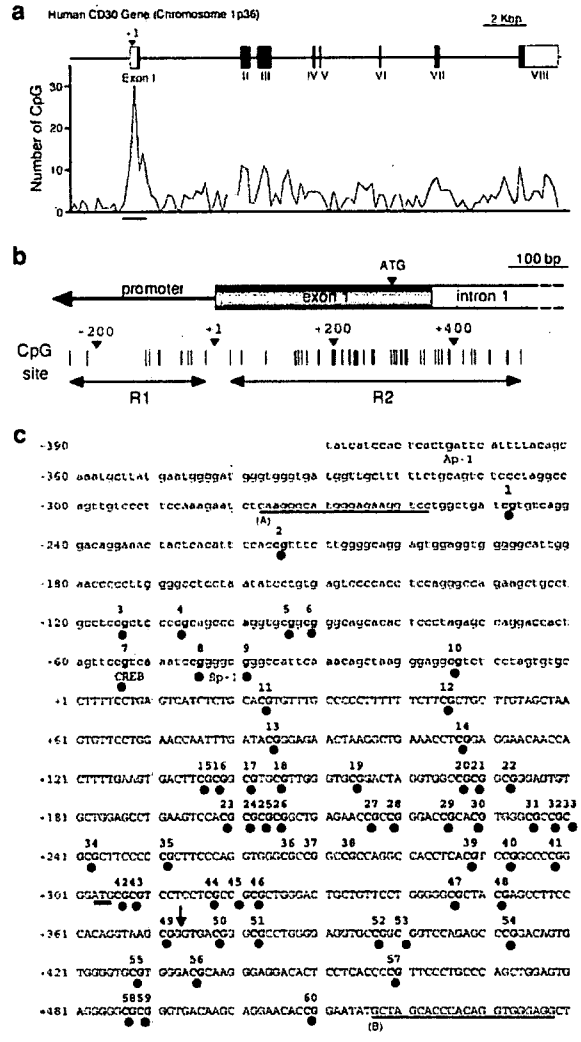

Figure 1 Map of CpG methylation sites in the promoter, exon 1 and intron 1 of the CD30; primer design for bisulfite sequencing. (**a**) The line graph indicates the number of CpG sites per 200 nucleotides in the CD30 gene. The region analyzed is indicated by a horizontal line. (**b**) Individual CpG sites analyzed are indicated as vertical lines and numbered from 1 to 60. Two clusters of CpG sites are indicated as R1 and R2. (**c**) Sequence of the CD30 genomic region analyzed. CpG sites are indicated by closed circles and numbered. The 5′ transcription start site is designated as +1 and initiation codon (ATG) at + 303 is underlined. The primers for PCR are underlined (**a** and **b**). The border between exon 1 and intron 1 is indicated by an arrow. Guanine at the nucleotide sequence +168 was reported as cytosine in the original report.[31] Potential transcription factor-binding sites are indicated.

In Vitro Methylation and Reporter Gene Assays

Activities of the CD30 promoter were studied by transient reporter gene assays. CD30 genomic region (−272 ~ +531) or (−390 ~ +531) was amplified by PCR with Takara LA *Taq*

polymerase using genomic DNA extracted from KMH2 cells and introduced into an *MluI*/*Hin*dIII site of pGL3Basic vector (Promega). Constructs were methylated *in vitro* with CpG Methylase (S.ssI) as recommended by the manufacture (New England Biolabs, Ipswich, MA, USA). The methylation status was checked by digestion with restriction enzymes *Hap*II and *Hha*I. Renilla luciferase expression vector driven by the herpes simplex virus thymidine kinase promoter, pRL-TK (Promega), was co-transfected to standardize transfection efficiency in each experiment. Luciferase activities were measured by Dual Luciferase assay kit (Promega). Transfection was carried out using Lipofectamine 2000 Reagent (Invitrogen) according to the manufacture's instructions.

Laser Capture Microdissection, DNA Extraction and Bisulfite Treatment of Clinical Samples

Formalin-fixed, paraffin-embedded sections were prepared from diagnostic biopsy samples of patients after informed consent. H–RS cells and ALCL cells, which were identified by staining with anti-CD30 antibody Ber-H2 (DAKO) and hematoxylin were microdissected using consecutive sections with modest staining by hematoxylin alone. Briefly, sections were dipped in xylene for 20 min, three changes of xylene for 20 s, three changes of 100% ethanol for 20 s, dipped in distilled water, three changes of 100% ethanol for 30 s and three changes of xylene for 20 s each. The sections were stained with hematoxylin lightly and after air-drying for 60 min, cells were microdissected using ARCTURUS LM200 Laser Capture Microdissection (LCM) unit (ARCTURUS, Mountain View, CA, USA) or Leica AS LMD microsystem (Leica Microsystems, Tokyo, Japan). DNA was extracted from microdissected samples after digestion with the PicoPure DNA Extraction Kit (ARCTURUS) followed by extraction with phenol–chloroform and precipitation with ethanol. Next, bisulfite-modified analysis was performed by MethylEasy DNA Bisulfite Modification Kit (Human Genetic Signatures Pty Ltd, Australia).

Statistical Analysis

Differences between mean values were assessed by two-tailed *t*-test. A *P*-value <0.05 was considered to be statistically significant.

Gene Bank Accession Number

The National Center for Biotechnology Information human genome sequence for CD30 is AJ 272029.

RESULTS

Identification of CpG Islands within the Core Promoter, First Exon and Intron of the CD30 Gene

Methylation of CpG islands located within the promoter region is one mechanism of epigenetic gene regulation. In order to address whether CD30 gene can be regulated epigenetically by CpG methylation, we analyzed the CpG sites in the 5′-region of CD30 gene. The analysis revealed CpG-rich sequences encompassing 60 CpG dinucleotides expanding a region within the promoter, the first exon and the first intron of the CD30 gene (Figure 1a). We identified two CpG islands (island R1, −249 to −15; island R2, +23 to +509). We deduced that CpG dinucleotides, 1–10 (from $-249\sim-15$) are located within the core promoter region and CpG dinucleotides, 11–60 are located within the first exon and a part of the first intron of CD30 gene (from $+23\sim+509$) (Figure 1b). Primers designed for PCR to amplify the 816 bp sequence that encompasses these 60 CpG sites were underlined (A and B in Figure 1c). Bisulfite sequencing was used to study the methylation status of each CpG site within this region.

Expression of CD30 mRNA and Proteins in H–RS, ALCL and Unrelated Cell Lines

We first examined the expression of CD30 mRNA and protein in H–RS cell lines (L428, KMH2, HDLM2, L540 and HDMYZ), ALCL cell lines (SUDHL1 and Karpas299) and unrelated cell lines used in this study. Unrelated cell lines examined include Jurkat (T-cell lymphoblastic lymphoma/leukemia), K562, ML1 and ML2 (all myeloid leukemia), HEK293 (embryonic kidney), FL (embryonal epithelium), HeLa (uterine cervical carcinoma) and A549 (lung adenocarcinoma). Among cell lines tested, all H–RS cell lines, except for HDMYZ, and all ALCL cell lines showed strong CD30 mRNA and protein expression. Among unrelated cell lines, Jurkat and K562 expressed lower levels of CD30 than H–RS or ALCL cells. Cell lines HeLa, ML1, ML2, HEK293, FL and A549 did not express CD30 (Figure 2a). These observations are in agreement with previous observations that CD30 is strongly expressed in H–RS and ALCL cells and absent or expressed at low levels in some hematopoietic cells, and not expressed in most nonhematopoietic cells.[5] Although HDMYZ is reported as a H–RS cell line, this cell line lacks several characteristics of H–RS cells including lack of CD30 expression.

Methylation Status of CD30 CpG Islands in H–RS, ALCL and Unrelated Cell Lines

In order to map the methylation sites within the CD30 CpG islands, we treated DNA from H–RS cell lines, ALCL cell lines and unrelated cell lines with bisulfite, which chemically converts unmethylated cytosine to uracil, whereas it has no effect on methylated cytosine, that is in CpG. PCR amplification, cloning and sequencing of bisulfite DNA showed a specific methylation pattern of the analyzed 60 CpG sites in all cell lines (Figure 2b and Table 1). In general, methylation status could be classified into cell lines with rarely methylated CD30 CpG islands (L428, KMH2, L540, HDLM2, Karpas299 and SUDHL1), those with frequently methylated CD30 CpG islands (HeLa ML1, ML2, HEK293, FL and A549) and those with partially methylated CD30 CpG islands (HDMYZ, Jurkat and K562). Interestingly, all cell lines with rarely methylated CD30 CpG islands were derived from HL or

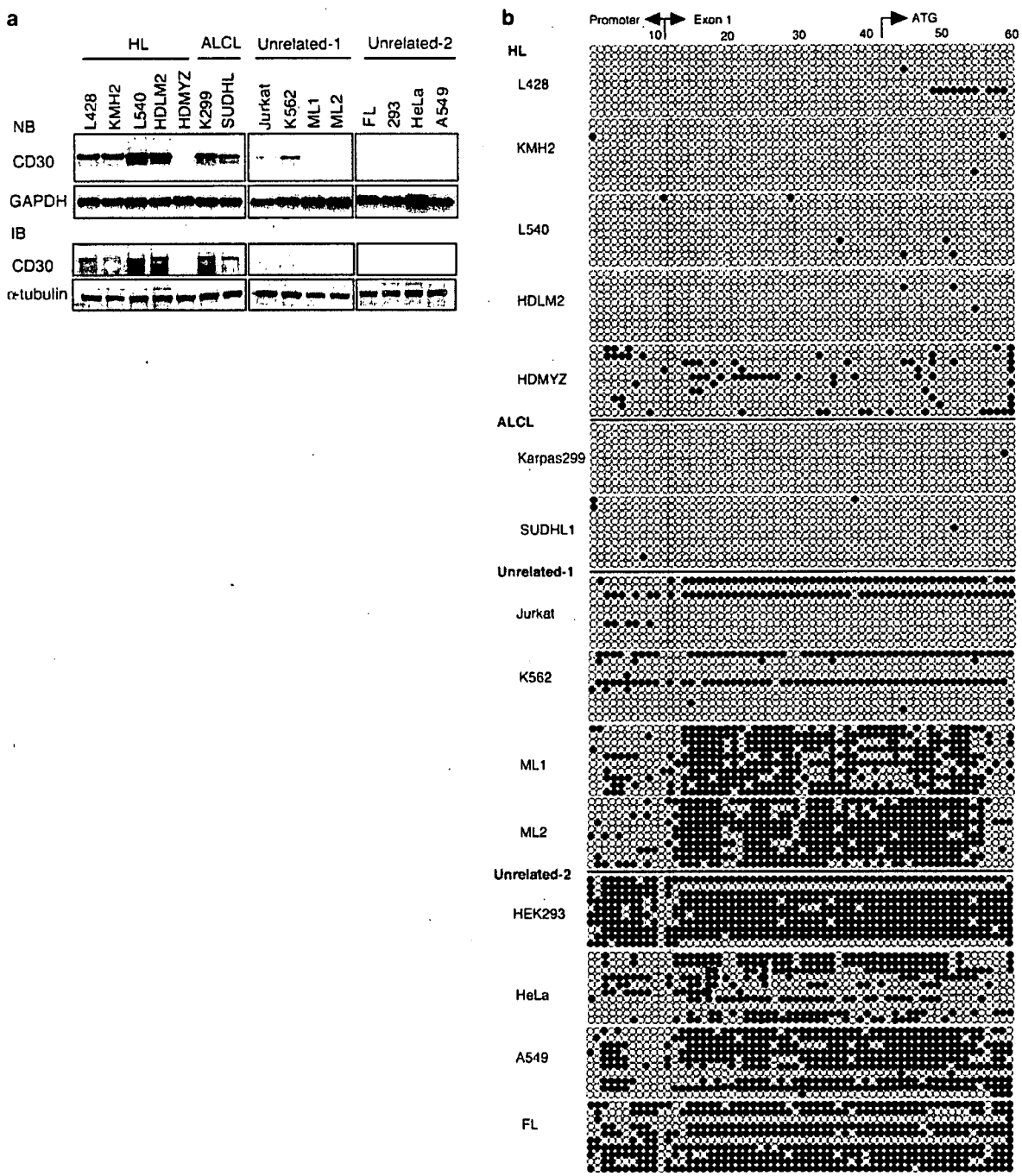

Figure 2 The expression level of CD30 and the status of CD30 CpG island methylation in H–RS, ALCL and unrelated cell lines. (**a**) Northern blot analysis of CD30. One microgram of polyadenylic acid-selected RNA was subjected to analysis. Glyceraldehyde-3-phosphate dehydrogenase (GAPDH) served as a control (top). Immunoblot analysis of CD30. Twenty micrograms of whole-cell lysates were subjected to analysis. Alpha tubulin served as a control (bottom). Cell lines used are indicated above the lanes. NB, northern blot analysis; IB, immunoblot analysis. (**b**) Results of bisulfite genomic sequencing coupled with TA cloning are shown. The methylation status of 10 clones for each sample is presented. Each circle represents a CpG site, a filled circle indicates methylation and an open circle indicates no methylation. Cell lines used are indicated on the left. The numbers described above correspond to those indicated in Figure 1.

ALCL, which are strongly CD30 positive. The percentage of CpG methylation in CD30 CpG islands from CD30-positive cells was very low (mean 5.3%) as compared with CD30-negative cells (mean 55.1%) and statistically significant ($P<0.01$) (Table 1). These results indicate involvement of CpG methylation in the regulation of CD30 expression.

Table 1 Methylation pattern of CD30 CpG islands

Cell lines	CD30	Methylated CpG (%)		
		Total	R1	R2
L428	+	1.8	0.0	2.2
KMH2	+	0.5	1.0	0.4
L540	+	1.0	0.0	1.2
HDLM2	+	0.5	0.0	0.6
Karpas299	+	0.2	0.0	0.2
SUDHL1	+	0.8	3.0	0.4
Jurkat	+	17.7	12.0	18.8
K562	+	19.7	23.0	19.0
Mean		5.3	4.9	5.3
HDMYZ	−	11.8	13.0	11.6
ML1	−	58.9	21.0	66.2
ML2	−	66.3	17.0	76.2
A549	−	60.3	29.0	70.2
HeLa	−	42.8	22.0	47.0
HEK293	−	76.8	85.0	66.6
FL	−	68.8	62.0	75.2
Mean		55.1	35.6	59.0

+, positive; −, negative; total, R1+R2.

Methylated CpG (%) = (number of CpG sites methylated/total CpG sites) × 100.

The data presented are average of 10 clones analysed. R1 and R2 are indicated in Figure 1.

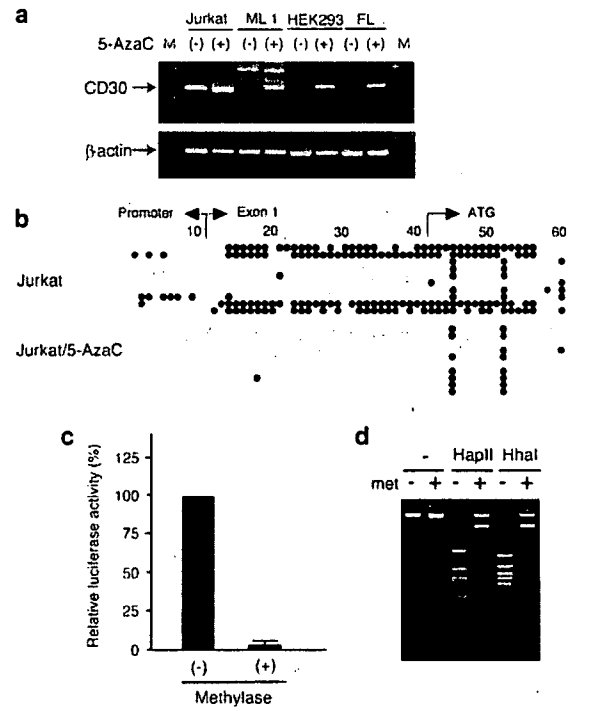

Figure 3 Regulation of CD30 expression by methylation. (**a**) Induction of CD30 expression after demethylation by 5-AzaC. Cells were treated with 5-AzaC at 1 μM (Jurkat) or 2 μM (ML1, HEK293, and FL) for 72 h at 37°C in a 5% CO_2 humidified atmosphere. Then, 5-AzaC was removed and cells were cultured for 48 h. Using cDNA obtained from these cell lines, the difference in expression level of CD30 mRNA transcripts without (−) or with (+) 5-AzaC treatment was examined by RT-PCR. After 35 cycles of amplification, products were analyzed by 3% agarose gel electrophoresis. (**b**) Representative methylation patterns of CD30 CpG islands in Jurkat lymphoblastic cells before and after 5-Aza C treatment. (**c**) Effect of introduction of methylation in transcriptional control of the CD30 promoter. Reporter gene assays were carried out using Jurkat cells and reporter plasmid containing CD30 CpG islands (−272 to +531 in Figure 1c) treated with or without S.ssI methylase. Relative activity of CD30 promoter treated with S.ssI methylase is shown. Activity of untreated CD30 promoter served as a control, which was set to 100%. (**d**) Restriction analysis of the methylated reporter construct. The construct before and after methylation was digested with methylation-sensitive endonucleases (*Hap*II and *Hha*I).

Among cell lines with frequently methylated CD30 CpG islands, relatively low frequency of methylation of R1 (promoter region) was found in ML1, ML2, HeLa and A549 (mean 22.3%), whereas methylation of R1 region frequency was high in HEK293 and FL (mean 73.5%) (Figure 2b and Table 1). Methylaton frequency of CpG sites within R2 (intron 1 and exon1) is almost equally high in these six cell lines.

Methylation of CD30 CpG Islands Decreases the Expression of CD30

To further examine whether methylation status of CD30 CpG islands affects the expression of CD30, we treated cell lines with modest CD30 expression (Jurkat) and cell lines without CD30 expression (ML1, HEK293 and FL) by 5-AzaC, which inhibits *de novo* and maintenance methylation. Treatment with 5-AzaC increased CD30 mRNA expression in cell lines with modest CD30 mRNA expression (Figure 3a). Notably, treatment with 5-AzaC induced CD30 mRNA expression in cell lines (ML1, HEK293 and FL) without constitutive CD30 expression (Figure 3a). Analysis of the methylation status of CD30 CpG islands in Jurkat revealed decreased CpG methylation levels after 5-AzaC treatment (Figure 3b). These observations indicate that decreased methylation status triggers expression of CD30. To provide evidence for the direct effect of methylation on CD30 promoter activity, we performed a reporter gene assay with CD30 promoter constructs (nucleic acid position at −276 ~ +531 in Figure 1c) before and after *in vitro* methylation. Treatment with S.ssI methylase significantly reduced transcriptional activity of the CD30 promoter, suggesting that the introduction of methylation suppresses activity of the CD30 promoter (Figure 3c). Methylation of the construct was confirmed by enzyme restriction assay (Figure 3d). These observations indicate that methylation of CD30 CpG islands reduces the expression of CD30.

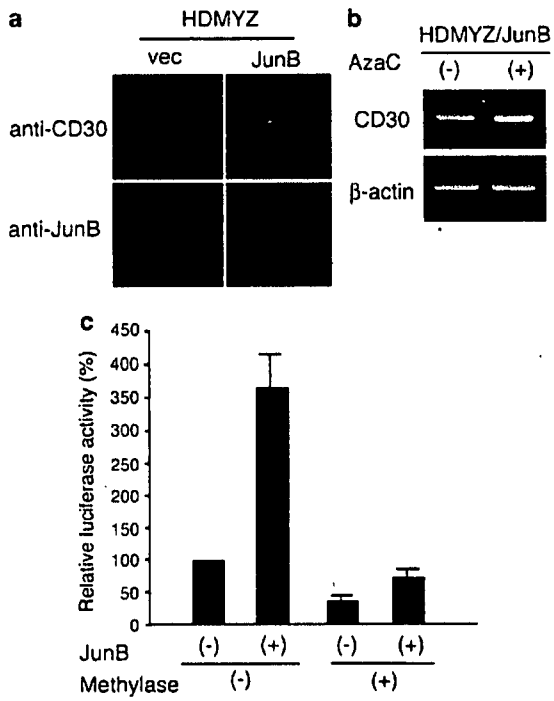

Figure 4 Roles of JunB and methylation status of CD30 GpG islands in CD30 induction. (**a**) Induction of CD30 in HDMYZ cells with stably transduced JunB. HDMYZ cells (1×10^7) were transfected with 5 μg of JunB expression vector or vacant vector using Lipofectoamine 2000 (Invitrogen) and selected by 3 μg/ml of puromycin. Cells cloned were stained with antibodies for CD30 and JunB and analyzed by confocal microscopy. (**b**) Induction of CD30 expression after 5-AzaC treatment. HDMYZ cells constitutively overexpressing JunB were treated with 5-AzaC at 1 μM for 72 h at 37°C in a 5% CO_2 humidified atmosphere. Then, 5-AzaC was removed and cells were cultured for 48 h. Using cDNA obtained from cells, the difference in expression level of CD30 mRNA transcripts without (−) or with (+) 5-AzaC treatment was examined by RT-PCR. After 35 cycles of amplification, products were analyzed by 3% agarose gel electrophoresis. β-Actin served as a control. (**c**) Effect of introduction of methylation in JunB-mediated induction of the CD30 promoter. Reporter gene assays were carried out using HDMYZ cells and 0.2 μg of reporter plasmid containing CD30 CpG islands of CD30 gene (−390 ~ + 531 in Figure 1c) treated with or without S.ssI methylase. In total, 0.5 μg of JunB or vacant vector was transfected based on the method described in the Materials and methods. Relative activity of CD30 promoter is shown. Activity of unmethylated CD30 promoter without JunB transfection served as a control, which was set to 100%.

JunB Action on the Demethylated CD30 Promoter Enhances CD30 Induction

We recently reported that JunB plays an important role in CD30 induction.[14] Therefore, we examined the effect of CD30 CpG island methylation on JunB-mediated induction of the CD30 promoter. For this purpose we used HDMYZ cells, whose CD30 CpG islands are partially methylated. HDMYZ lacks CD30 expression (Figure 2a) and shows weak JunB expression (data not shown). We produced transformants of HDMYZ cells overexpressing JunB and three independent clones were examined for CD30 expression. Constitutive overexpression of JunB in HDMYZ cells induced CD30, and 5-Aza C treatment of these clones enhanced CD30 expression. Representative results are shown in Figure 4a and b, respectively. The results indicate that JunB-mediated induction of CD30 is enhanced by reduced methylation status of the CD30 promoter. To confirm the above result, we performed a gene reporter assay with CD30 promoter constructs (nucleic acid position at −390 ~ + 531 in Figure 1c) before and after *in vitro* methylation. JunB-mediated CD30 promoter induction was abolished when the CD30 promoter treated with S.ssI methylase was used (Figure 4c). The result suggests that constitutive action of overexpressed JunB on reduced methylation of CD30 CpG islands enhances CD30 promoter induction.

Status of CD30 CpG Island Methylation, JunB and CD30 Expression in H–RS Cells, ALCL Cells and Normal Lymphocytes

To obtain insight into CD30 induction during transformation of nonmalignant lymphocytes to H–RS and ALCL cells, we examined the methylation status of CD30 CpG islands in H–RS cells, ALCL cells and normal lymphocytes. For this purpose, H–RS cells, ALCL cells and nonmalignant germinal center (GC) cells were microdissected from tissue biopsy samples ($n = 3$ for each). PBMC from healthy volunteers were also studied ($n = 3$). We also examined the expression of CD30 and JunB in HL, ALCL, nonmalignant GC and PBMC by immunostaining ($n = 5$ for each). CD30 CpG islands of H–RS cells, ALCL cells, GC cells and PBMC were rarely methylated. CD30 and JunB were strongly positive in H–RS and ALCL cells, whereas CD30 and JunB were negative in GC cells of tonsils and PBMC. Representative results are shown in Figure 5a and b. These results indicate that both JunB expression and hypomethylation of CpG islands are required for CD30 expression.

DISCUSSION

Methylation of CpG islands located in gene promoter regions is thought to be one mechanism of gene regulation. For example, aberrant CpG methylation of the SHP-1 promoter occurs in the pathogenesis of both B- and T-cell lymphomas.[17,18] Therefore, we investigated the methylation status of the CD30 promoter, since CD30 overexpression is essential to the pathogenesis of HL and ALCL.[6,9,19] We identified CpG islands encompassing 60 CpG dinucleotides, located in the core promoter, exon 1 and intron 1 of CD30 gene. Our observations in various cell lines reveal that methylation of this region inversely correlates with expression of CD30, suggesting that the CpG methylation inhibits CD30 expression. This conclusion is supported by the results that treatment with demethylating agent 5-AzaC increases CD30 expression in cell lines with high CpG methylation, and CpG methylation of the CD30 promoter by S.ssI methylase decreases transcriptional activity of CD30 promoter.

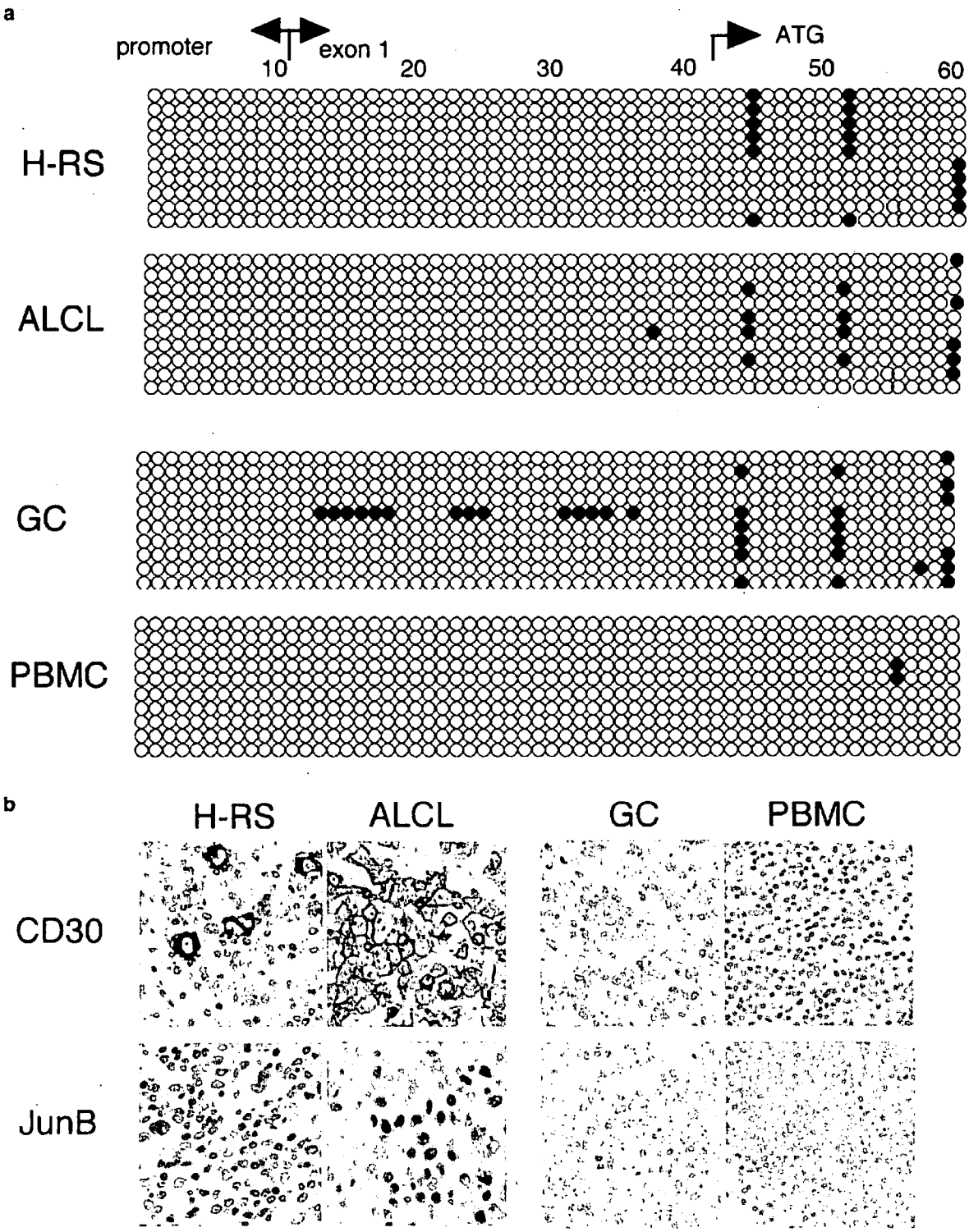

Figure 5 Status of CD30 CpG islands methylation and JunB expression in H–RS cells, ALCL cells and lymphocytes. (**a**) Analysis of H–RS cells, ALCL cells and GC cells of normal tonsils obtained by microdissection and PBMC by bisulfite genomic sequencing coupled with TA cloning. The methylation status of 10 clones for each sample is represented. Each circle represents a CpG site, a filled circle indicates methylation and an open circle indicates no methylation. Cells used are indicated on the left. The numbers above correspond to those indicated in Figure 1. (**b**) Expression of JunB and CD30 in H–RS cells, ALCL cells, GC cells and PBMC. Tissue samples (HL, ALCL and normal tonsil) and normal PBMC were stained with antibodies for CD30 (top) or JunB (bottom).

Analysis of the methylation pattern of cell lines with frequently methylated CD30 CpG islands (Figure 2b) indicates that low methylation frequency of CpG sites within R2 (exon 1 and intron 1) is significant for CD30 expression. On the other hand, the R1 (core promoter) contains GC box and CREB-binding motifs. These motifs in general initiate and promote transcription by recruiting general transcription factors and coactivators.[20] It has been demonstrated that DNA methylation can interfere with protein–DNA interactions, recruitment of histone deacetylases, and the induction of chromatin condensation necessary for gene inactivation. Several methyl-binding proteins can compete with transcription factors for the same sequences.[21,22] Therefore, it is likely that the methylation frequency of CpG sites within R1 is also critical for CD30 expression. In sum, low methylation frequency of CpG sites within both R1 and R2 regions appear to be necessary for CD30 induction.

We show that both hypomethylation of CD30 CpG islands and strong JunB expression are required for enhanced CD30 expression. We reported that CD30 overexpression in H–RS cells and ALCL cells is caused by strong AP-1 activity of JunB. Interaction of JunB with the AP-1 site in the CD30 promoter, which is situated upstream of the R1 region, drives CD30 expression.[14] However, JunB alone failed to recover activity of the CD30 promoter treated by S.ssI methylase (Figure 4c). JunB overexpression in cell lines with partial methylation could induce CD30 expression which was enhanced by 5-AzaC treatment (Figure 4a and b). Together, these results support the conclusion that both hypomethylation of CD30 CpG islands and JunB overexpression enhance CD30 expression.

Based on the results that the methylation status of CD30 CpG islands critically affect CD30 expression, we hypothesized that CD30 CpG islands in normal germinal center cells and peripheral lymphocytes are methylated and demethylation events directly trigger constitutive CD30 induction. However, our results show that CD30 CpG islands of normal lymphocytes are rarely methylated, suggesting that demethylation of CD30 CpG islands is not sufficient to trigger CD30 induction during lymphomagenesis. Instead, our current results indicate that aberrant induction of JunB at hypomethylated CD30 CpG islands triggers CD30 induction and initiates an autocrine loop of CD30-mediated activation of NF-κB and ERK1/2-MAPK in HL and ALCL.[9]

DNA hypomethylation and mismatch repair deficiency interact to cause invasive T- and B-cell lymphomas in mice.[23] The exact mechanism for lymphogenesis in these mice is unknown, although enhanced microsatellite instability is likely to be involved.[24] In the case of HL and ALCL, which are derived from B- and T lymphocytes, microsatellite instability is uncommon.[25,26] Instead, we found initiation and constitutive transcription of CD30 gene by aberrant JunB expression maintains hypomethylation of CD30 CpG islands and contributes to the transformation of lymphocytes to H–RS and ALCL cells. Previous reports support the notion that constitutive transcription of genes inhibits the progression of their methylation.[27–30]

In conclusion, the results of this study indicate that the methylation status of CD30 CpG islands and expression level of JunB together are responsible for high CD30 expression. Combined with our recent findings, these results suggest that constitutive action of JunB on hypomethylated CD30 CpG islands in lymphocytes triggers CD30 induction and initiates high constitutive activity of a JunB-CD30-JunB loop, maintaining hypomethylation of CD30 CpG islands and contributing to the pathogenesis of HL and ALCL.

ACKNOWLEDGEMENT

This work was supported by Grants-in-Aid for Scientific Research from Japanese Society for Promotion of Science and a grant from The Mochida Memorial Foundation for Medical and Pharmaceutical Research to Ryouichi Horie.

1. Schwab U, Stein H, Gerdes J, *et al.* Production of a monoclonal antibody specific for Hodgkin and Sternberg–Reed cells of Hodgkin's disease and a subset of normal lymphoid cells. Nature 1982;299:65–67.
2. Smith CA, Gruss HJ, Davis T, *et al.* CD30 antigen, a marker for Hodgkin's lymphoma, is a receptor whose ligand defines an emerging family of cytokines with homology to TNF. Cell 1993;73:1349–1360.
3. Durkop H, Latza U, Hummel M, *et al.* Molecular cloning and expression of a new member of the nerve growth factor receptor family that is characteristic for Hodgkin's disease. Cell 1992;68:421–427.
4. Falini B, Pileri S, Pizzolo G, *et al.* CD30 (Ki-1) molecule: a new cytokine receptor of the tumor necrosis factor receptor superfamily as a tool for diagnosis and immunotherapy. Blood 1995;85:1–14.
5. Horie R, Watanabe T. CD30: expression and function in health and disease. Semin Immunol 1998;10:457–470.
6. Horie R, Watanabe T, Morishita Y, *et al.* Ligand-independent signaling by overexpressed CD30 drives NF-kappaB activation in Hodgkin–Reed–Sternberg cells. Oncogene 2002;21:2493–2503.
7. Horie R, Watanabe T, Ito K, *et al.* Cytoplasmic aggregation of TRAF2 and TRAF5 proteins in the Hodgkin–Reed–Sternberg cells. Am J Pathol 2002;160:1647–1654.
8. Nonaka M, Horie R, Itoh K, *et al.* Aberrant NF-kappaB2/p52 expression in Hodgkin/Reed–Sternberg cells and CD30-transformed rat fibroblasts. Oncogene 2005;24:3976–3986.
9. Watanabe M, Sasaki M, Itoh K, *et al.* JunB induced by constitutive CD30-extracellular signal-regulated kinase 1/2 mitogen-activated protein kinase signaling activates the CD30 promoter in anaplastic large cell lymphoma and Reed–Sternberg cells of Hodgkin lymphoma. Cancer Res 2005;65:7628–7634.
10. Seitz V, Hummel M, Marafioti T, *et al.* Detection of clonal T-cell receptor gamma-chain gene rearrangements in Reed–Sternberg cells of classic Hodgkin disease. Blood 2000;95:3020–3024.
11. Kanzler H, Kuppers R, Hansmann ML, *et al.* Hodgkin and Reed–Sternberg cells in Hodgkin's disease represent the outgrowth of a dominant tumor clone derived from (crippled) germinal center B cells. J Exp Med 1996;184:1495–1505.
12. Croager EJ, Gout AM, Abraham LJ. Involvement of Sp1 and microsatellite repressor sequences in the transcriptional control of the human CD30 gene. Am J Pathol 2000;156:1723–1731.
13. Croager EJ, Muir TM, Abraham LJ. Analysis of the human and mouse promoter region of the non-Hodgkin's lymphoma-associated CD30 gene. J Interferon Cytokine Res 1998;18:915–920.
14. Watanabe M, Ogawa Y, Ito K, *et al.* AP-1 mediated relief of repressive activity of the CD30 promoter microsatellite in Hodgkin and Reed–Sternberg cells. Am J Pathol 2003;163:633–641.
15. Horie R, Ito K, Tatewaki M, *et al.* A variant CD30 protein lacking extracellular and transmembrane domains is induced in HL-60 by tetradecanoylphorbol acetate and is expressed in alveolar macrophages. Blood 1996;88:2422–2432.
16. Clark SJ, Harrison J, Paul CL, *et al.* High sensitivity mapping of methylated cytosines. Nucleic Acids Res 1994;22:2990–2997.

17. Koyama M, Oka T, Ouchida M, *et al.* Activated proliferation of B-cell lymphomas/leukemias with the SHP1 gene silencing by aberrant CpG methylation. Lab Invest 2003;83:1849–1858.
18. Zhang Q, Wang HY, Marzec M, *et al.* STAT3- and DNA methyltransferase 1-mediated epigenetic silencing of SHP-1 tyrosine phosphatase tumor suppressor gene in malignant T lymphocytes. Proc Natl Acad Sci USA 2005;102:6948–6953.
19. Horie R, Watanabe M, Ishida T, *et al.* The NPM-ALK oncoprotein abrogates CD30 signaling and constitutive NF-kappaB activation in anaplastic large cell lymphoma. Cancer Cell 2004;5:353–364.
20. Philipsen S, Suske G. A tale of three fingers: the family of mammalian Sp/XKLF transcription factors. Nucleic Acids Res 1999;27:2991–3000.
21. Johnson CA, Turner BM. Histone deacetylases: complex transducers of nuclear signals. Semin Cell Dev Biol 1999;10:179–188.
22. Garinis GA, Patrinos GP, Spanakis NE, *et al.* DNA hypermethylation: when tumour suppressor genes go silent. Hum Genet 2002;111:115–127.
23. Trinh BN, Long TI, Nickel AE, *et al.* DNA methyltransferase deficiency modifies cancer susceptibility in mice lacking DNA mismatch repair. Mol Cell Biol 2002;22:2906–2917.
24. Kim M, Trinh BN, Long TI, *et al.* Dnmt1 deficiency leads to enhanced microsatellite instability in mouse embryonic stem cells. Nucleic Acids Res 2004;32:5742–5749.
25. Hodges KB, Vnencak-Jones CL, Larson RS, *et al.* Rarity of genomic instability in pathogenesis of systemic anaplastic large cell lymphoma (ALCL) in immunocompetent patients. Hum Pathol 1999;30:173–177.
26. Re D, Benenson L, Wickenhauser C, *et al.* Proficient mismatch repair protein expression in Hodgkin and Reed Sternberg cells. Int J Cancer 2002;97:205–210.
27. De Smet C, Loriot A, Boon T. Promoter-dependent mechanism leading to selective hypomethylation within the 5′ region of gene MAGE-A1 in tumor cells. Mol Cell Biol 2004;24:4781–4790.
28. Song JZ, Stirzaker C, Harrison J, *et al.* Hypermethylation trigger of the glutathione-*S*-transferase gene (GSTP1) in prostate cancer cells. Oncogene 2002;21:1048–1061.
29. Miyamoto K, Fukutomi T, Akashi-Tanaka S, *et al.* Identification of 20 genes aberrantly methylated in human breast cancers. Int J Cancer 2005;116:407–414.
30. Hagihara A, Miyamoto K, Furuta J, *et al.* Identification of 27 5′ CpG islands aberrantly methylated and 13 genes silenced in human pancreatic cancers. Oncogene 2004;23:8705–8710.
31. Durkop H, Oberbarnscheidt M, Latza U, *et al.* Structure of the Hodgkin's lymphoma-associated human CD30 gene and the influence of a microsatellite region on its expression in CD30 (+) cell lines. Biochim Biophys Acta 2001;1519:185–191.

Leukemia (2007) 21, 992–997

www.nature.com/leu

ORIGINAL ARTICLE

Unbalanced translocation der(1;7)(q10;p10) defines a unique clinicopathological subgroup of myeloid neoplasms

M Sanada[1,7], N Uike[2], K Ohyashiki[3], K Ozawa[4], W Lili[1], A Hangaishi[5], Y Kanda[5], S Chiba[6], M Kurokawa[5], M Omine[7], K Mitani[8] and S Ogawa[1,9]

[1]Department of Regeneration Medicine for Hematopoiesis, Graduate School of Medicine, University of Tokyo, Tokyo, Japan; [2]Department of Hematology/Oncology, National Kyushu Cancer Center, Fukuoka, Japan; [3]Department of Hematology, Tokyo Medical University, Tokyo, Japan; [4]Department of Hematology, Jichi Medical School, Tochigi, Japan; [5]Department of Hematology/Oncology, Graduate School of Medicine, University of Tokyo, Tokyo, Japan; [6]Cell Therapy and Transplantation Medicine, Graduate School of Medicine, University of Tokyo, Tokyo, Japan; [7]Division of Hematology, Internal Medicine, Showa University Fujigaoka Hospital, Yokohama, Japan; [8]Department of Hematology, Dokkyo University School of Medicine, Tochigi, Japan and [9]Core Research for Evolutional Science and Technology, Japan Science and Technology Agency, Saitama, Japan

The unbalanced translocation, der(1;7)(q10;p10), is one of the characteristic cytogenetic abnormalities found in myelodysplastic syndromes (MDS) and other myeloid neoplasms. Although described frequently with very poor clinical outcome and possible relationship with monosomy 7 or 7q- (−7/7q-), this recurrent cytogenetic abnormality has not been explored fully. Here we analyzed retrospectively 77 cases with der(1;7)(q10;p10) in terms of their clinical and cytogenetic features, comparing with other 46 adult −7/7q- cases without der(1;7)(q10;p10). In contrast with other −7/7q- cases, where the abnormality tends to be found in one or more partial karyotypes, der(1;7)(q10;p10) represents the abnormality common to all the abnormal clones and usually appears as a sole chromosomal abnormality during the entire clinical courses, or if not, is accompanied only by a limited number and variety of additional abnormalities, mostly trisomy 8 and/or loss of 20q. der(1;7)(q10;p10)-positive MDS cases showed lower blast counts ($P<0.0001$) and higher hemoglobin concentrations ($P<0.0075$) at diagnosis and slower progression to acute myeloid leukemia ($P=0.0043$) than other −7/7q- cases. der(1;7)(q10;p10) cases showed significantly better clinical outcome than other −7/7q cases ($P<0.0001$). In conclusion, der(1;7)(q10;p10) defines a discrete entity among myeloid neoplasms, showing unique clinical and cytogenetic characteristics.

Leukemia (2007) **21**, 992–997. doi:10.1038/sj.leu.2404619; published online 22 February 2007
Keywords: MDS; AML; MPD; t(1;7); cytogenetics

Introduction

The unbalanced translocation, der(1;7)(q10;p10), is a nonrandom chromosomal abnormality found in myelodysplastic syndromes (MDS) as well as acute myeloid leukemia (AML), and less frequently in myeloproliferative disorders (MPD).[1] It is presented typically with an International System for Chromosome Nomenclature (2005) description,[2] 46,XY(or XX), +1,der(1;7)(q10;p10) and characterized by the presence of one of the two possible derivative chromosomes with two copies of apparently normal chromosome 1 and a single copy of the intact chromosome 7, leading to allelic imbalance of trisomy 1q and monosomy 7q. It was found consistently in 1.5–6% in MDS, 0.2–2.1% in AML and rarely in MPD depending on the literature.[3–9] Detailed molecular studies using quantitative fluorescent *in situ* hybridization analysis disclosed that the translocation is likely to occur through a mitotic recombination within the large clusters of homologous centromere alphoid sequences, D1Z7 on chromosome 1 and D7Z1 on chromosome 7. The breakpoints are widely distributed within these alphoids clusters but typically spare the short arm third of both alphoids, suggesting that it may not be a dicentric chromosome but that der(1;7)(q10,q10) is a more appropriate karyotypic description for this translocation.[10]

On the other hand, however, the clinical aspect of this translocation is less clearly defined compared with its genomic structure. While the common clinical features thus far reported include a previous history of chemo- and/or radiotherapies in more than half cases,[11–13] presence of eosinophilia,[13] trilineage dysplasia, high rates of progression to AML in MDS cases and poor prognosis with less than 1 year of median survival,[3,14,15] these features have not been fully investigated because of the rarity of this translocation compared with other well-characterized cytogenetic groups found in AML/MDS. Also it is unclear that its pathogenetic link to monosomy 7 or partial deletion of 7q (−7/7q-) other than der(1;7)(q10;p10), although some authors speculated that der(1;7)(q10;p10) represents a mere variant of the former.

In this paper, to clarify these points, we analyzed retrospectively 77 cases with der(1;7)(q10;p10) for their clinical and genetic/cytogenetic characteristics in comparison with other 46 cases with −7/7q-. A literary review of 125 der(1;7)(q10;p10) cases was also provided.

Materials and methods

Patients

The patients included in this study are those who were diagnosed and treated as having MDS, AML and MPD at one of the collaborating hospitals during 1 January 1990 through 30 September 2005, for whom at least one cytogenetic report showed either der(1;7)(q10;p10), monosomy 7, or other unbalanced abnormalities showing loss of genetic materials of the long arm of chromosome 7. −7/7q- was required to be

Correspondence: Dr S Ogawa, Department of Hematology and Oncology, Department of Regeneration Medicine for Hematopoiesis, Graduate School of Medicine, University of Tokyo, 7-3-1, Hongo, Bunkyo-ku, Tokyo 113-8655, Japan.
E-mail: sogawa-tky@umin.ac.jp
Received 24 August 2006; revised 25 January 2007; accepted 25 January 2007; published online 22 February 2007